Junction Loss Experiments: Laboratory Report

U.S. Department of Transportation
Federal Highway Administration

Foreword

The junction loss study described in this report was conducted at the Federal Highway Administration (FHWA) hydraulics laboratory. Between 1986 and 1992, Chang et al. conducted a lab study of energy losses through junction access holes, using relatively large-scale (one-quarter scale) physical models.[1] A preliminary method for determining such losses, based on early results from that study, was published in the Federal Highway Administration's (FHWA) *Urban Drainage Design Manual* (Hydraulic Engineering Circular No. 22 (HEC 22)).[2] FHWA plans to update HEC 22 and further develop computer software for storm drain design. The need for consistent technology in FHWA publications and software applications on this subject is urgent. To accommodate that need and overcome some of the difficulties in estimating energy loss in access holes, the FHWA's Office of Bridge Technology initiated this study to validate Roger Kilgore's proposed method for computing access hole energy losses. This report will be of interest to hydraulic engineers involved in storm drain design and to researchers involved in developing improved storm drain design guidelines. It is being published as a Web document only.

Gary L. Henderson, P.E.
Director, Office of Infrastructure
Research and Development

Notice

This document is disseminated under the sponsorship of the U.S. Department of Transportation in the interest of information exchange. The U.S. Government assumes no liability for the use of the information contained in this document. This report does not constitute a standard, specification, or regulation.

The U.S. Government does not endorse products or manufacturers. Trademarks or manufacturers' names appear in this report only because they are considered essential to the objective of the document.

Quality Assurance Statement

The Federal Highway Administration (FHWA) provides high-quality information to serve Government, industry, and the public in a manner that promotes public understanding. Standards and policies are used to ensure and maximize the quality, objectivity, utility, and integrity of its information. FHWA periodically reviews quality issues and adjusts its programs and processes to ensure continuous quality improvement.

Technical Report Documentation Page

1. Report No. FHWA-HRT-07-036	2. Government Accession No.	3. Recipient's Catalog No. N/A
4. Title and Subtitle Junction Loss Experiments: Laboratory Report		5. Report Date March 2007
		6. Performing Organization Code N/A
7. Author(s) Kornel Kerenyi, J. Sterling Jones, and Stuart Stein		8. Performing Organization Report No. N/A
9. Performing Organization Name and Address GKY and Associates, Inc. 5411-E Backlick Road Springfield, VA 22151		10. Work Unit No. (TRAIS) N/A
		11. Contract or Grant No. DTFH-04-C-00037
12. Sponsoring Agency Name and Address Office of Infrastructure Research and Development Federal Highway Administration 6300 Georgetown Pike McLean, VA 22101-2296		13. Type of Report and Period Covered Laboratory Report March 2004–May 2006
		14. Sponsoring Agency Code FHWA Task Order 10

16. Abstract

The current study has two objectives. The first is to evaluate Roger Kilgore's proposed procedure, which requires conducting some of the same types of tests that were run in the previous study. The new tests conducted include a wider range of parameters, such as greater plunge-height ratios and steeper pipe slopes. Previous research was limited in that it was applicable to storm drain systems located only in relatively flat areas; the research would not hold up for systems in hilly and mountainous regions of the country where steep pipe slopes are the norm.

The second and more challenging objective is to characterize the energy level in an access hole. If that can be accomplished, then the familiar culvert hydraulics analyses can be applied to the access hole that serves as the tailbox where inflow pipes enter and to the headbox for outflow pipes where the water exits. Researchers have attempted numerous analyses of particle image velocimetry (PIV) data and three-dimensional (3–D) numerical model data, with uneven results. Characterizing energy in the access hole is highly problematic because the flow is so chaotic, and arbitrary assumptions had to be made to obtain results that fall between intuitive limits. Researchers at the FHWA lab now have investigated the more organized flow in the contracted area of the outflow pipe, using the contraction ratio as an indirect measure of the contraction loss in the flow from the access hole to the outflow pipe to backcalculate the energy loss in the access hole.

17. Key Words Energy loss, junction loss, storm drain, access hole, manhole, hydraulics, physical model.	18. Distribution Statement No restrictions. This document is available to the public through the National Technical Information Service (NTIS), Springfield, VA 22161.		
19. Security Classif. (of this report) Unclassified	20. Security Classif. (of this page) Unclassified	21. No. of Pages 63	22. Price

Form DOT F 1700.7 (8-72) Reproduction of completed page authorized

SI* (MODERN METRIC) CONVERSION FACTORS

APPROXIMATE CONVERSIONS TO SI UNITS

Symbol	When You Know	Multiply By	To Find	Symbol
LENGTH				
in	inches	25.4	millimeters	mm
ft	feet	0.305	meters	m
yd	yards	0.914	meters	m
mi	miles	1.61	kilometers	km
AREA				
in^2	square inches	645.2	square millimeters	mm^2
ft^2	square feet	0.093	square meters	m^2
yd^2	square yard	0.836	square meters	m^2
ac	acres	0.405	hectares	ha
mi^2	square miles	2.59	square kilometers	km^2
VOLUME				
fl oz	fluid ounces	29.57	milliliters	mL
gal	gallons	3.785	liters	L
ft^3	cubic feet	0.028	cubic meters	m^3
yd^3	cubic yards	0.765	cubic meters	m^3
NOTE: volumes greater than 1000 L shall be shown in m^3				
MASS				
oz	ounces	28.35	grams	g
lb	pounds	0.454	kilograms	kg
T	short tons (2000 lb)	0.907	megagrams (or "metric ton")	Mg (or "t")
TEMPERATURE (exact degrees)				
^oF	Fahrenheit	5 (F-32)/9 or (F-32)/1.8	Celsius	^oC
ILLUMINATION				
fc	foot-candles	10.76	lux	lx
fl	foot-Lamberts	3.426	candela/m^2	cd/m^2
FORCE and PRESSURE or STRESS				
lbf	poundforce	4.45	newtons	N
lbf/in^2	poundforce per square inch	6.89	kilopascals	kPa

APPROXIMATE CONVERSIONS FROM SI UNITS

Symbol	When You Know	Multiply By	To Find	Symbol
LENGTH				
mm	millimeters	0.039	inches	in
m	meters	3.28	feet	ft
m	meters	1.09	yards	yd
km	kilometers	0.621	miles	mi
AREA				
mm^2	square millimeters	0.0016	square inches	in^2
m^2	square meters	10.764	square feet	ft^2
m^2	square meters	1.195	square yards	yd^2
ha	hectares	2.47	acres	ac
km^2	square kilometers	0.386	square miles	mi^2
VOLUME				
mL	milliliters	0.034	fluid ounces	fl oz
L	liters	0.264	gallons	gal
m^3	cubic meters	35.314	cubic feet	ft^3
m^3	cubic meters	1.307	cubic yards	yd^3
MASS				
g	grams	0.035	ounces	oz
kg	kilograms	2.202	pounds	lb
Mg (or "t")	megagrams (or "metric ton")	1.103	short tons (2000 lb)	T
TEMPERATURE (exact degrees)				
^oC	Celsius	1.8C+32	Fahrenheit	^oF
ILLUMINATION				
lx	lux	0.0929	foot-candles	fc
cd/m^2	candela/m^2	0.2919	foot-Lamberts	fl
FORCE and PRESSURE or STRESS				
N	newtons	0.225	poundforce	lbf
kPa	kilopascals	0.145	poundforce per square inch	lbf/in^2

*SI is the symbol for the International System of Units. Appropriate rounding should be made to comply with Section 4 of ASTM E380.
(Revised March 2003)

TABLE OF CONTENTS

LIST OF FIGURES

iv

LIST OF TABLES

LIST OF SYMBOLS

A	area (m^2 (ft^2)).
A_c	contracted area (m^2 (ft^2)).
A_o	cross-sectional area of the outlet pipe (m^2 (ft^2)).
A_k	cross-sectional area associated with a contour of velocity (m^2 (ft^2)).
b	access hole or junction chamber diameter (m (ft)).
C	energy loss coefficient (dimensionless).
C_B	energy loss coefficient for benching (dimensionless).
C_θ	energy loss coefficient for angled inflow (dimensionless).
C_H	energy loss coefficient for plunging inflow (dimensionless).
D_I	discharge intensity (dimensionless).
D_o	outlet pipe diameter (m (ft)).
E_a	final calculated energy level (m (ft)).
E_{a1}	initial energy level in the access hole (m (ft)).
$E_{a,ff}$	estimated access hole energy level for full flow (m (ft)).
$E_{a,ics}$	estimated access hole energy level for submerged inlet control (m (ft)).
$E_{a,icu}$	estimated access hole energy level for unsubmerged inlet control (m (ft)).
E_i	energy at the inlet (m (ft)).
E_o	total energy calculated for the upstream end of the outlet pipe (m (ft)).
ΔE	additional energy loss for ΔE_B, ΔE_θ, and ΔE_H (m (ft)).
ΔE_B	additional energy loss for benching (floor configuration) (m (ft)).
ΔE_θ	additional energy loss for angled inflows other than 180 degrees (m (ft)).
ΔE_H	additional energy loss for plunging flows (m (ft)).
ΔE_i	exit energy loss (m (ft)).
ΔE_{oc}	energy loss in the outflow pipe (m (ft)).
$H_{L,i}$	inflow loss (m (ft)).
$H_{L,o}$	outflow loss (m (ft)).
H_k	plunge height (m (ft)).
g	acceleration due to gravity (m/s^2 (ft/s^2)).
K_i	exit loss coefficient (dimensionless).
K_o	entrance loss coefficient (dimensionless).
P_o/γ	outlet pressure head (m (ft)).
Q	flow (m^3/s (ft^3/s)).
Q_i	inlet flow (m^3/s (ft^3/s)).
Qj	nonplunging inflow (m^3/s (ft^3/s)).
Q_k	plunging inflow (m^3/s (ft^3/s)).
Q_o	Outlet flow (m^3/s (ft^3/s)).
V_i	inflow velocity (m/s (ft/s)).
V_o	outflow velocity (m/s (ft/s)).
$V_o^2/2g$	outlet velocity head (m).
y_a	water depth (m (ft)).
y_{a1}	estimated structure water depth (m (ft)).
y_o	outlet flow depth (m (ft)).
z_k	plunging inlet elevation (m (ft)).
z_o	outlet pipe invert elevation (m (ft)).
γ	specific weight of water (N/m^3 (lb/ft^3)).

θ_j inflow angle (degrees).
θ_w flow-weighted angle (degrees).

ABBREVIATED GLOSSARY

CCD   charge coupled device.
CIS   contact image sensors.
EGL   energy grade line.
HEC   Hydraulic Engineering Circular.
HGL   hydraulic grade line.
PIV   particle image velocimetry.

1. INTRODUCTION

BACKGROUND

Storm drains generally collect storm runoff from streets, parking lots, and other structures and convey this water to a desired outfall. Access holes (or manholes), which allow staff to inspect, maintain, or repair a segment of the drainage, are usually spaced about 92 to 183 meters (m) (300 to 600 feet (ft)) apart along a given pipe and at every junction between multiple pipes. An access hole, which has at least one inlet pipe and one outlet pipe intersecting it, is usually constructed from a vertically oriented concrete pipe or box that is large enough for a person to enter by removing the cast iron lid and using a ladder (see figure 1). In addition to allowing access, access hole junctions also allow pipes to easily change one or more variables: direction, slope, diameter, and elevation.

Figure 1. Photo. Typical access hole.

Estimating the energy loss associated with these access hole junctions is a critical step in designing a drainage network that can handle the incoming flow from various storm events (see figure 2). Between 1986 and 1992, Chang et al. conducted a lab study of energy losses through junction access holes, using relatively large-scale (one-quarter scale) physical models.[1] A

1

preliminary method for determining such losses, based on early results from that study, was published in the Federal Highway Administration's (FHWA) *Urban Drainage Design Manual* (Hydraulic Engineering Circular No. 22 (HEC 22)).[2] A revised method, based on the final results, was coded in the highway drainage (HYDRAIN) software system.[3]
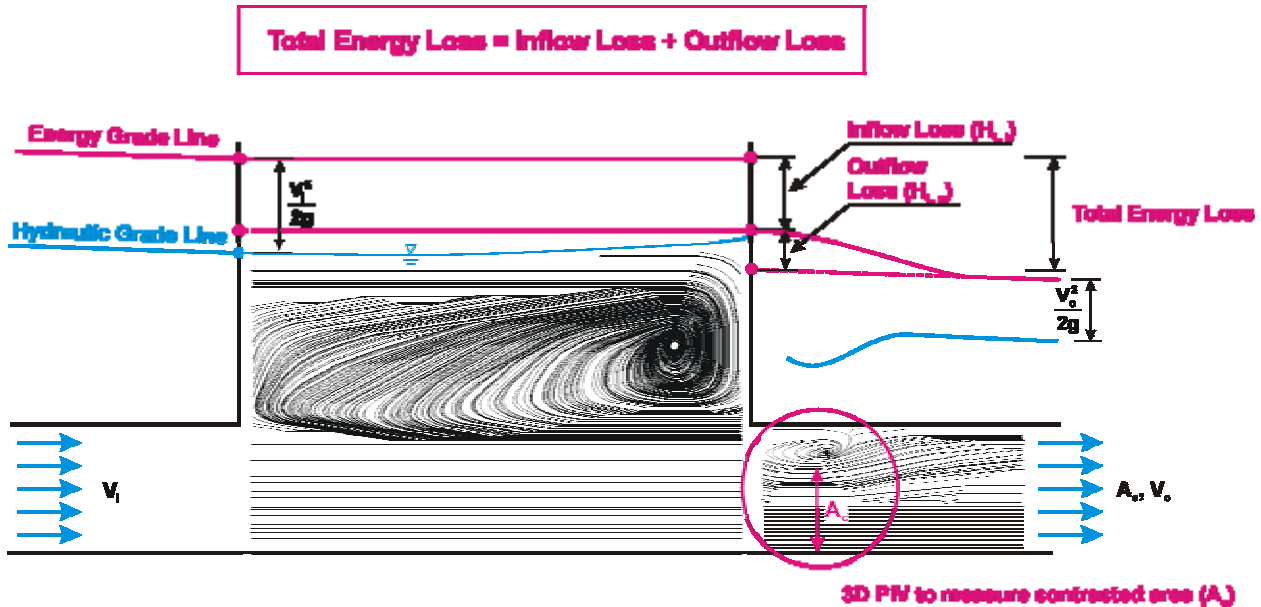
Figure 2. Diagram. Cross-section definition sketch of an access hole.

Practitioners questioned both of these methods when they encountered situations beyond the range of the experimental parameters tested in the lab study. They found that these methods have limitations when applied to junctions with plunging inflow and to junctions with outflow pipes that carry supercritical flow. These methods are also relatively complex and require iterative solutions. A criticism of both the HEC 22 and HYDRAIN approaches is that they use the same loss coefficient for different flow conditions.[2,3]

These issues ultimately motivated the FHWA to reanalyze the old lab data. Roger Kilgore of Kilgore Consulting and Management, who was the principal investigator in this effort, developed a new method that classifies access holes and their hydraulic conditions in a manner similar to the way that culverts are classified as "inlet controlled" or "full flow." The primary hypothesis of this method is that the energy loss coefficient should be a function of the basic flow conditions in an access hole. The result is a new method, which is somewhat simpler than the existing methods and might improve handling of plunging flow and supercritical flow situations.

Kilgore initially tested his new method using the 1986–1992 lab data by separating the data into two groups. The first group consisted of "base runs" with the simplest configurations (one inflow and one outflow pipe with the same base elevations) to establish first approximations of the energy loss across an access hole. The second group included the more complex lab configurations entailing benching, angled inflows, and plunging inflows. Kilgore used the second group of experiments to derive adjustments to the first approximations. All of the theory behind these approximations will be given in the theory section later in this report. Kilgore's analysis of the old lab data, however, was concurrently supplemented with additional lab experiments

conducted by the FHWA Hydraulics Laboratory. This report summarizes the additional experiments and the data collected and used to evaluate the new junction loss methodology.

PROBLEM

The previous research was limited to relatively flat storm drain systems. The results were presented as empirical equations that were not readily understood from intuitive reasoning, and the methods in HEC-22 and in the HYDRAIN computer program were not consistent.[2,3] For these reasons, the research in this report has two main objectives. The first is to evaluate the proposed junction loss method by conducting new tests that are very similar to the previous study. The new tests, however, include a wider range of parameters, such as greater plunge-height ratios and steeper pipe slopes. The second and more challenging objective is to characterize the energy level in an access hole with various inflow and outflow pipe configurations using local measurements of velocity and pressure head. Characterizing the energy level in an access hole is highly problematic because the flow is so chaotic, and a certain degree of trial and error is required to interpret the laboratory data in a way that practitioners will find useful.

This new laboratory data was shared with Kilgore, who subsequently modified part of his methodology to accommodate the new results. The FHWA and Kilgore agreed on the following experiments to evaluate his proposed procedure.

1. Fifteen base runs with discharge intensity (D_I) varying from 0.2 and 1.3, and average access hole depth between 4 and 12 centimeters (cm) (1.8 to 4.7 inches) (i.e. full flow). One level inflow pipe should be oriented at 180°, and the outflow pipe should be level with a b/D_o ratio of 4.

2. Eighteen runs with an outflow pipe slope that induces supercritical flow. In one case, the inflow pipe should be oriented at 180°. In the second case, the inflow pipe should be oriented at 90°. In the third case, two inflow pipes should be oriented on a level floor with Q_{i1} at 180° and Q_{i2} at 90° with equal flow rates in each inflow pipe. The outflow discharge (Q_o) should be varied so that there are three submerged and three unsubmerged cases with a discharge intensity (D_I) never exceeding 1.98 (e.g., D_I equal to 0.36, 0.54, 0.72, 1.08, 1.44, 1.8).

3. Eighteen runs with plunging inflow. One level inflow pipe should be oriented 180°, one plunging inflow pipe (Q_k) should be oriented 90°, and the outflow pipe (Q_o) should be level with a b/D_o ratio of 4. The following characteristics should also be included:

   a. All runs should have the same outflow (Q_o) with D_I equal to 0.72.
   b. The plunging inlet elevation, z_k, should be varied: $3D_o$, $5D_o$, and $10D_o$.
   c. The fraction of flow coming from the plunging inlet should be varied so that Q_k/Q_o equals 0.25, 0.5, and 0.75.
   d. Since D_o is constant, the tailwater should be controlled so that E_a equals $1.5D_o$ and $3.0D_o$.

D_I is calculated by equation 1.

$$D_I = \frac{Q}{A\sqrt{gD_o}}$$

(1)

2. THEORY

Kilgore's proposed method for calculating the energy loss across an access hole has three fundamental steps.[4]

1. Determine an initial access hole energy level, E_{a1}, based on "inlet controlled" flow conditions (i.e., weir and orifice) or "full flow" conditions.

2. Adjust the initial access hole energy level for benching, inflow angle(s), and plunging flows to compute the final calculated energy level, E_a.

3. Calculate the exit loss from each inflow pipe and estimate the energy gradeline, E_i, which will then be used to continue calculations upstream.

These three steps are illustrated in figure 3.
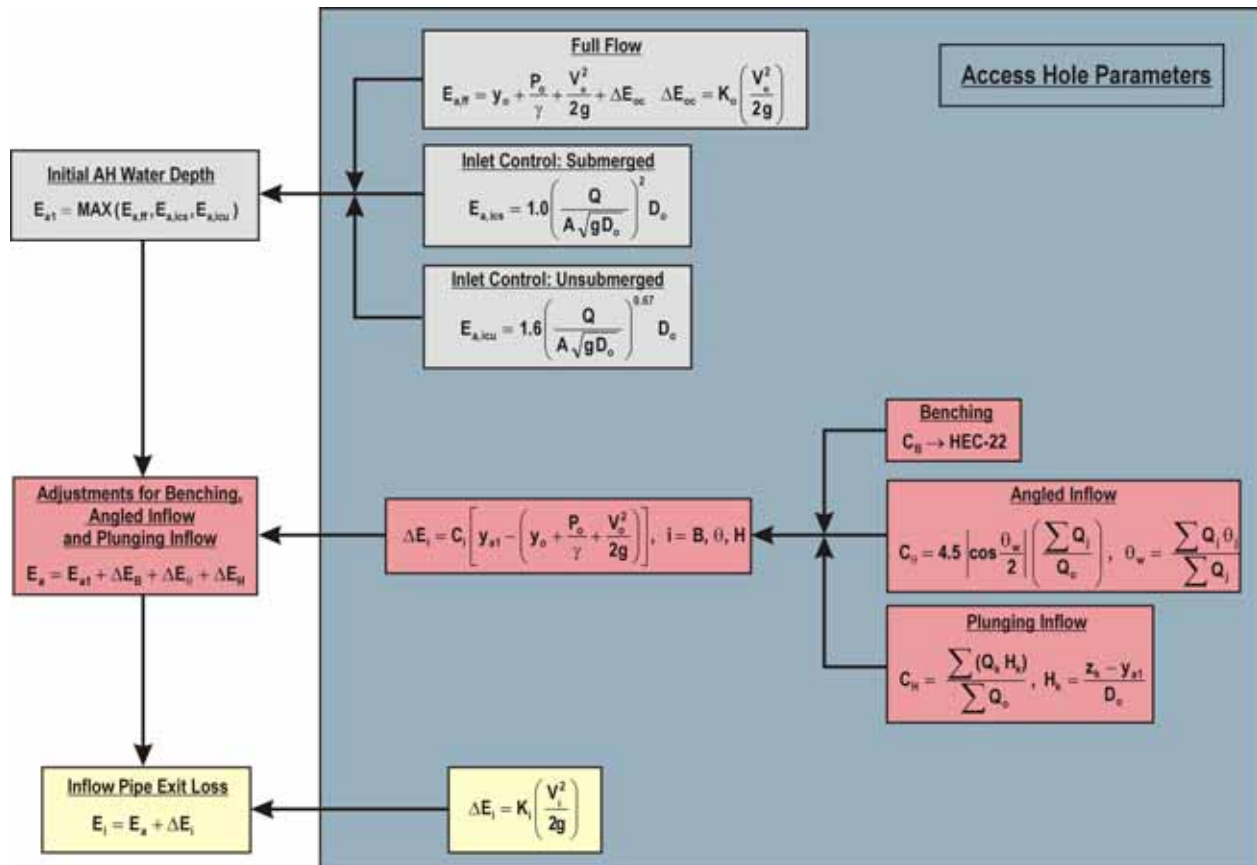
Figure 3. Diagram. Flow chart for the proposed junction loss method.

5

INITIAL ACCESS HOLE ENERGY LEVEL

The initial energy level in the access hole structure, E_{a1}, is calculated as the maximum of three possible conditions; these determine the hydraulic regime within the structure. The three conditions considered for the outlet pipe are full flow, submerged inlet control, and unsubmerged inlet control. A fourth condition, partially full outlet control, could occur but was not pursued because it was not considered to be a practical limiting condition in storm drain design.

The full flow condition is considered when the outlet pipe is flowing full. This is a common occurrence when a storm drain system is surcharged and may also occur if flow in the pipe is limited by pipe capacity. The submerged inlet control condition occurs if flow is limited by the opening in the access hole structure to the outlet pipe rather than by the pipe capacity, and the resulting water depth in the access hole is sufficiently high that flow through the opening can be analyzed by orifice flow equations. The unsubmerged inlet control condition is also limited by the opening, but the resulting water level in the access hole is lower and weir flow equations can be used. The initial estimate of energy level is taken as the maximum of the three potential values (equation 2).

$$E_{a1} = \max(E_{a,ff}, E_{a,ics}, E_{a,icu}) \tag{2}$$

In this equation:

$E_{a,ff}$ is estimated access hole energy level for full flow.
$E_{a,ics}$ is estimated access hole energy level for submerged inlet control.
$E_{a,icu}$ is estimated access hole energy level for unsubmerged inlet control.

The full flow computation uses velocity head, but full flow only applies when the outlet pipe is flowing full. The two inlet control estimates depend only on discharge and pipe diameter. This is important because velocity is not a reliable parameter for the following reasons:

- In cases where supercritical flow occurs in the outlet pipe, flow in the outlet pipe (and the corresponding velocity head) are defined by the upstream condition at the access hole rather than the velocity head determining upstream conditions.

- In the laboratory setting, velocity is not directly measured. It is calculated from depth and the continuity relationship. Small errors in depth measurement can result in large variations in velocity head.

- Velocities produced in laboratory experiments are the result of localized hydraulic conditions, which are not necessarily representative of the velocities calculated based on equilibrium pipe hydraulics in storm drain computations.

Full Flow

In the full flow condition, discharge into the access hole is limited by surcharges in the downstream storm drain system such that the outflow pipe is flowing full. Using a culvert analogy, this is one of the potential cases of outlet control. In this case, the initial structure energy level is estimated by the equation 3.

$$E_{a,ff} = y_o + \frac{P_o}{\gamma} + \frac{V_o^2}{2g} + \Delta E_{oc} \tag{3}$$

The entrance loss assuming outlet control, ΔE_{oc}, is calculated by equation 4.

$$\Delta E_{oc} = K_o \left(\frac{V_o^2}{2g} \right) \tag{4}$$

In these equations:

g	is acceleration due to gravity (meters per second squared (m/s^2)).
Γ	is the specific weight of water (Newtons per cubic meters (N/m^3)).
y_o	is outlet flow depth (m).
P_o/γ	is outlet pressure head (m).
$V_o^2/2g$	is outlet velocity head (m).
K_o	is the entrance loss coefficient, which is 0.2 and dimensionless.

Equations 3 and 4 are used only when the outlet flow depth (y_o) plus the outlet pressure head (P_o/γ) is greater than D_o, where D_o is the outlet pipe diameter; otherwise $E_{a,ff}$ is 0.0. The outlet pipe invert elevation (z_o) is the datum for this analysis, and is set to zero. Equation 3 estimates energy level directly without considering the water surface within the access hole. Defining a one-dimensional velocity head in a location where highly turbulent multidirectional flow may exist presents a challenge. Marsalek noted that the energy loss coefficient is unaffected by changes in the relative access hole diameter as long as the ratio of b over D_o ranges from 2 to 6.[5] Sangster's study showed that the energy loss coefficient is primarily affected when the ratio is less than 3.[6] The reanalyzed lab data, however, does not appear to support the need for a contraction factor such as the ratio of b over D_o.

Submerged Inlet Control

The inlet control calculations employ the dimensionless ratio adapted from the analysis of culverts that is referred to here as the discharge intensity (D_I). It is described by the ratio of discharge to pipe dimensions, where A is the area (equation 5).

$$D_I = \left(\frac{Q}{A\sqrt{gD_o}} \right) \tag{5}$$

The original submerged inlet control equation (equation 6) uses the analogy of inflow via a submerged orifice. Equation 6, however, should be limited to discharge intensities less than or equal to 1.6 because the reanalyzed data set did not include observations above this threshold.

$$E_{a,ics} = 1.2 \left(\frac{Q}{A\sqrt{gD_o}} \right)^2 D_o \tag{6}$$

Kilgore selected a coefficient equal to 1.2.[4] However, early lab experiments show that this coefficient should be about 1.0, instead of 1.2. Equation 7 is the revised equation.

$$E_{a,ics} = 1.0 \left(\frac{Q}{A\sqrt{gD_o}} \right)^2 D_o \tag{7}$$

Unsubmerged Inlet Control

The unsubmerged inlet control equation (equation 8) uses the analogy of inflow via a weir.

$$E_{a,icu} = 1.6 \left(\frac{Q}{A\sqrt{gD_o}} \right)^{0.67} D_o \tag{8}$$

The coefficients for equations 4, 6, 7, and 8 were empirically derived to achieve a best fit with the reanalyzed laboratory data. These coefficients are lower than comparable values for culverts as reported in Norman, et al.[7] Since conditions in an access hole differ from conditions at the inlet to a culvert, one would not expect an exact correspondence. What is apparent from the lab data, however, is that the change in access hole energy level is analogous to culverts.

ADJUSTMENTS FOR BENCHING, ANGLED INFLOW, AND PLUNGING INFLOW

The initial structure energy level calculated in the previous section is used as a basis for estimating additional losses for discharges entering the structure at angles other then 180°, benching configurations, and discharges entering the structure at elevations above the water depth in the access hole. Flows entering a structure from an inlet above the water surface in the access hole can be treated as plunging flows. The effects of these conditions may be estimated and applied to the initial access hole energy level using the principle of superposition. This additive approach avoids a problem experienced in other methods where unreasonable values of energy losses are obtained when a single multiplicative coefficient takes on an extreme value. The revised access hole energy level, E_a, equals the initial estimate modified by each of the three factors covered in this section, as shown in equation 9.

$$E_a = E_{a1} + (\Delta E_B + \Delta E_\theta + \Delta E_H) = E_{a1} + \Delta E \tag{9}$$

In this equation:

ΔE_B is additional energy loss for benching (floor configuration).
ΔE_θ is additional energy loss for angled inflows other than 180°.
ΔE_H is additional energy loss for plunging flows.
ΔE is additional energy loss for ΔE_B, ΔE_θ, and ΔE_H.

As described earlier, E_a represents the level of the energy grade line (EGL) in the access hole. However, if E_a is calculated to be less than E_o (the outlet energy level), then E_a should be set equal to E_o. Designers may also wish to know the water level in the access hole. A conservative approach would be to use E_a as y_a for design purposes. Traditional approaches to energy losses typically attempt to estimate all losses based on a single velocity head and for reasons described earlier the approach proposed in this paper is moving away from this strategy. The alternative proposed here is to estimate these additional energy losses as a function of the total energy losses computed between the access hole and the outlet pipe. The formulation in equation 10 expresses the additional losses, ΔE, as directly proportional to the energy loss estimated in the first step between the access hole and the outlet pipe.

$$\Delta E = C\left[E_{a1} - \left(y_o + \frac{P_o}{\gamma} + \frac{V_o^2}{2g}\right)\right] \tag{10}$$

In this equation, C is the energy loss coefficient—C_B, C_θ, or C_H—for benching, angled inflow, and plunging inflow, respectively. The term between the parentheses and beginning with y_o is the total energy, E_o, calculated for the upstream end of the outlet pipe.

Note that the final E_a value cannot be less than E_o, and that the bracketed terms in equation 10 must be nonnegative. Another difficulty with equation 10 concerns the outlet velocity head. When the entrance condition to the outlet pipe limits flow into the pipe (inlet control) or the outlet pipe is flowing in a supercritical flow condition, the outlet velocity head may not be representative of the energy losses occurring within the access hole for reasons described earlier. The derivation of C for each adjustment is addressed in the following subsections.

Benching

The reanalyzed lab data suggests that the correction factors reported by Chang et al. and HEC 22 for benching, after adapting them to the form of equation used in this methodology, needed some adjustment.[1,2] Table 1 summarizes the suggested values for C_B. A negative value indicates water depth will be reduced rather than increased.

9

Table 1. Values for the Coefficient C_B.

Floor Configuration	Bench Submerged*	Bench Unsubmerged*
Flat (level)	-0.05	-0.05
Depressed	0.0	0.0
Half Benched	-0.05	-0.85
Full Benched[†]	-0.25	-0.93
Improved[†]	-0.60	-0.98

* Submerged is E_{a1}/D_o greater than 2.5, and unsubmerged is E_{a1}/D_o less than 1.0. Linear interpolation between the two values is used for intermediate values.

[†] No evaluation or adjustments to these floor configurations have been made because these configurations were not included in the FHWA testing.

Angled Inflow

The effect of skewed inflows entering the structure is addressed with momentum vectors. To maintain simplicity in the method, the contributions (θ_j) from all of the nonplunging inflows are resolved into a single flow-weighted angle, θ_w (equation 11).

$$\theta_w = \frac{\sum Q_j \theta_j}{\sum Q_j} \tag{11}$$

The angles in the previous equation are measured from the outlet pipe (e.g., 180° is a straight pipe), and the summation only includes nonplunging flows as indicated by the subscript j. If all flows are plunging, θ_w is set to 180°. It does not matter whether the angle is defined in a clockwise or counterclockwise orientation as long as it is defined consistently. For example, if two pipes are entering the structure orthogonal to the outflow pipe, one must be designated as 90° and the other as 270° for the momentum vectors. The angled inflow coefficient is then calculated using equation 12.

$$C_\theta = 4.5 \left| \cos \frac{\theta_w}{2} \right| \left(\frac{\sum Q_j}{Q_o} \right) \tag{12}$$

Note that the angled inflow coefficient approaches zero as θ_w approaches 180° and the relative inflow approaches zero.

Plunging Inflow

Plunging inflow is defined as inflow (pipe or inlet) where the invert of the pipe, z_i, is greater than the estimated structure water depth, y_{a1} (taken as E_{a1} as an approximation). Several approaches were attempted to describe a parameter that captures the presumed effect of plunging height on energy losses in the access hole based on defining a plunge height. A balance between simplicity

and effectiveness was achieved by defining relative plunge height, H_k, for each plunging pipe, denoted by the subscript k (equation 13).

$$H_k = \frac{z_k - y_{a1}}{D_0}$$
(13)

Equation 13 was incorporated into a relationship for C_H (equation 14).

$$C_H = \left(\frac{\sum (Q_k H_k)}{Q_o} \right)$$
(14)

Note that as the proportion of plunging flows approaches zero, C_H also approaches zero. Equations 13 and 14 are limited to conditions where z_k is less than $10D_o$. If z_k is greater than $10D_o$, z_k should be set to $10D_o$.

INFLOW PIPE EXIT LOSSES

The final step is to calculate the EGL in each inflow pipe. Two cases must be considered. The first case is for nonplunging inflow pipes—that is, those pipes with a hydraulic connection to the water in the access hole. Inflow pipes operating under this condition are identified when E_a is greater than z_i. In these cases, the energy at the inlet, E_i, is backcalculated from the access hole energy level and the exit loss, ΔE_i (equation 15).

$$E_i = E_a + \Delta E_i$$
(15)

Since the criticality of the inflow does not influence the exit loss, the exit loss can be calculated in the traditional manner using the inflow pipe velocity head (equation 16).

$$\Delta E_i = K_i \left(\frac{V_i^2}{2g} \right)$$
(16)

In this equation, the exit loss coefficient, K_i, equals 0.4 and is dimensionless.

As was found in examining the entrance losses, the ratio of b over D_o was not a significant predictor of exit energy losses. The second case for an inflow pipe is a plunging condition. For pipes that are plunging, E_i is the EGL calculated from the inflow pipe hydraulics and will be approximately critical energy if the inlet pipe is on a subcritical slope.

The resulting energy level is used to continue computations upstream to the next access hole except when the inlet pipe is on a steep (supercritical) slope and is not submerged for its full length, in which case the hydraulics are controlled at the upstream end of the pipe.

Thus, the three-step procedure of estimating—first, entrance losses, then additional losses, and finally exit losses—is repeated at each access hole.

3. EXPERIMENTAL SETUP

The original 1986–1992 FHWA lab study, Chang et al., used a large-scale model of an access hole with a diameter of 0.6 m (2.0 ft), which is almost prototype scale for some applications (see figure 4).[1] The original study included 755 test runs. In the current study, a much smaller scale—a scaling ratio of 1 to 4—makes the experimental setup easier to operate. The new experimental equipment (see figure 5) involves higher precision instrumentation to investigate a wider range of parameters and a particle image velocimetry (PIV) technique to visualize and measure the flow patterns. The smaller scale also reduces the cost associated with the special tracer particles that are used in the PIV technique.

Figure 4. Photo. Access hole prototype in the 1986–1992 study with the lab technician to show relative size.
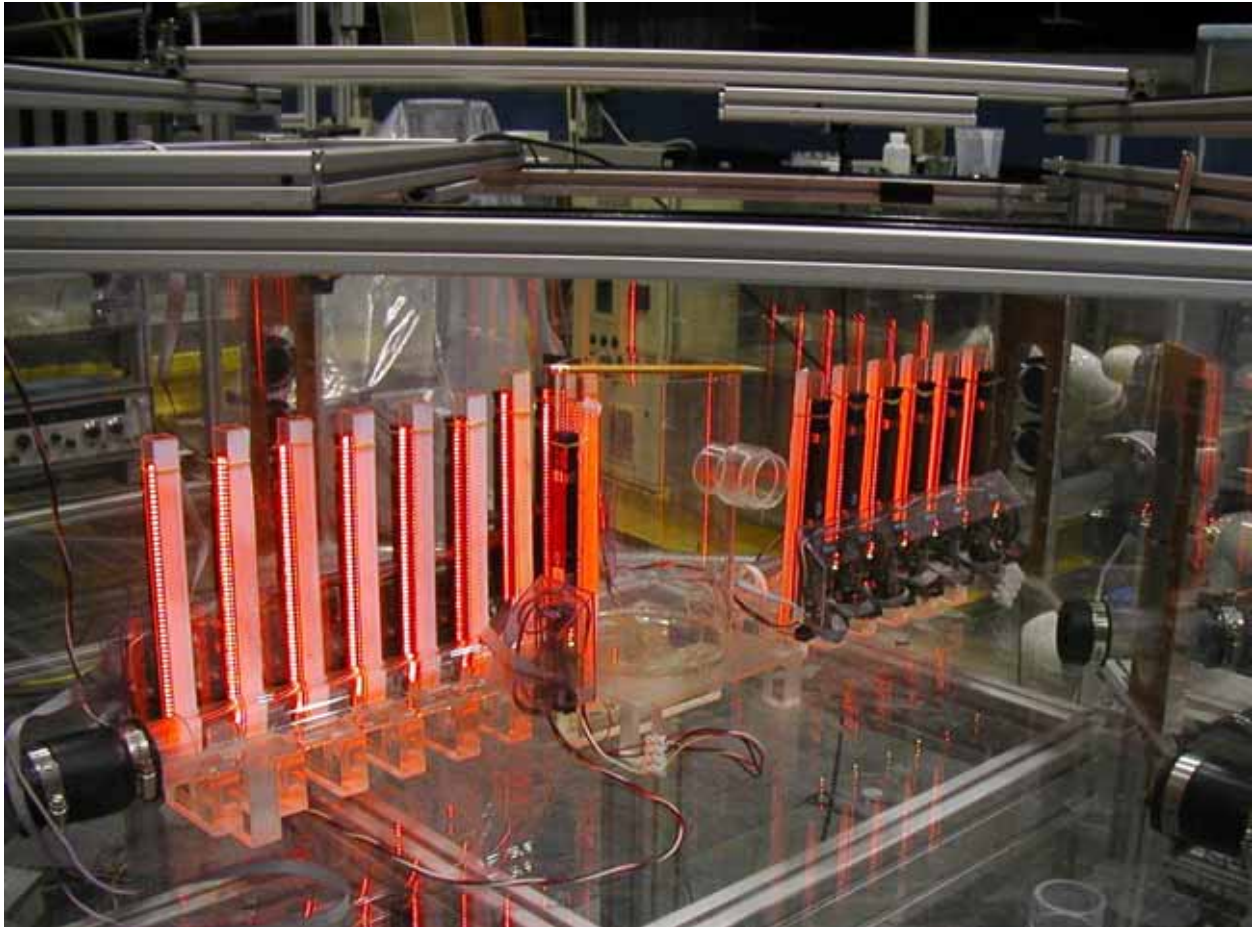
Figure 5. Photo. The scaled model of an access hole equipped with standpipe instruments.

The new test apparatus for junction energy loss includes three water tanks: a headbox, a main tank, and a tailbox. The purpose of the headbox tank is to control the pressure head for the experiments and to allow injection of seeding particles for the PIV technique. The junction loss model is mounted inside the main tank, where it is surrounded by still water to minimize distortions for the stereoscopic PIV recordings. The main tank also supports a carriage system for an ultrasonic sensor that measures the flow depth in the access hole junction. This setup is capable of maintaining a constant flow depth in the access hole during the test run, and the water in the standpipes measures the hydraulic grade line (HGL) in the inflow and outflow pipes. The tailbox tank is designed to control the tail water.

The measurements of the total loss through the access hole did not require measuring the energy inside the access hole. Two techniques were developed to measure the flow depth. One method used laser sensors to measure the distance down to a floating disk in each standpipe. Another method, recently developed at the FHWA Hydraulics Laboratory, uses contact image sensors (CIS) mounted on the sides of the standpipes to measure the water column in the stand pipes (see figures 5 and 6). The biggest advantage of the CIS system is that it measures the water columns in all of the standpipes simultaneously, which increases the precision of the loss coefficient calculation.
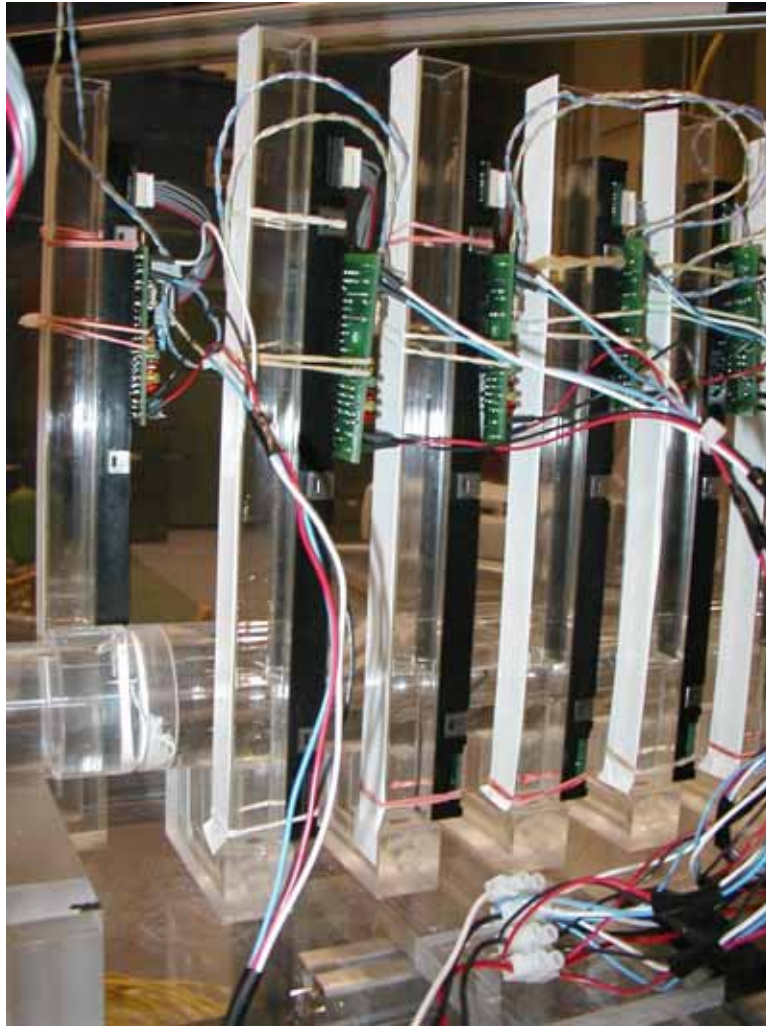
Figure 6. Photo. CIS sensors attached to standpipes.

Three flow meters provide discharge readings, which are used to compute velocity head. CIS sensors mounted at four locations in the access hole measure an average water surface elevation. All of the model pipes are fabricated from Plexiglas™. The access hole is 15 cm (6 inches) in diameter, and the inflow and outflow pipes are 3.8 cm (1.5 inches) in diameter, which yields a relative access hole diameter (i.e., b/D_o) equal to 4. The outflow pipe in the miniculvert experiments was 5.1 centimeters (2 inches) in diameter.

For reasons discussed in the results section, stereoscopic PIV techniques and 3–D numerical models were used to characterize the velocity profile at different locations (vertical slices) along the outflow pipe from the access hole (see figure 7) and from the miniculvert (see figure 8) setups. The PIV technique is an optical flow diagnostic based on the interaction of light refraction and scattering in non-homogeneous media. The fluid motion is made visible by tracking the locations of small tracer particles between two snapshots in time. The velocity flow field is inferred by plotting the particle displacements versus time. Thus, the PIV technique makes it possible to measure instantaneous velocity flow fields.
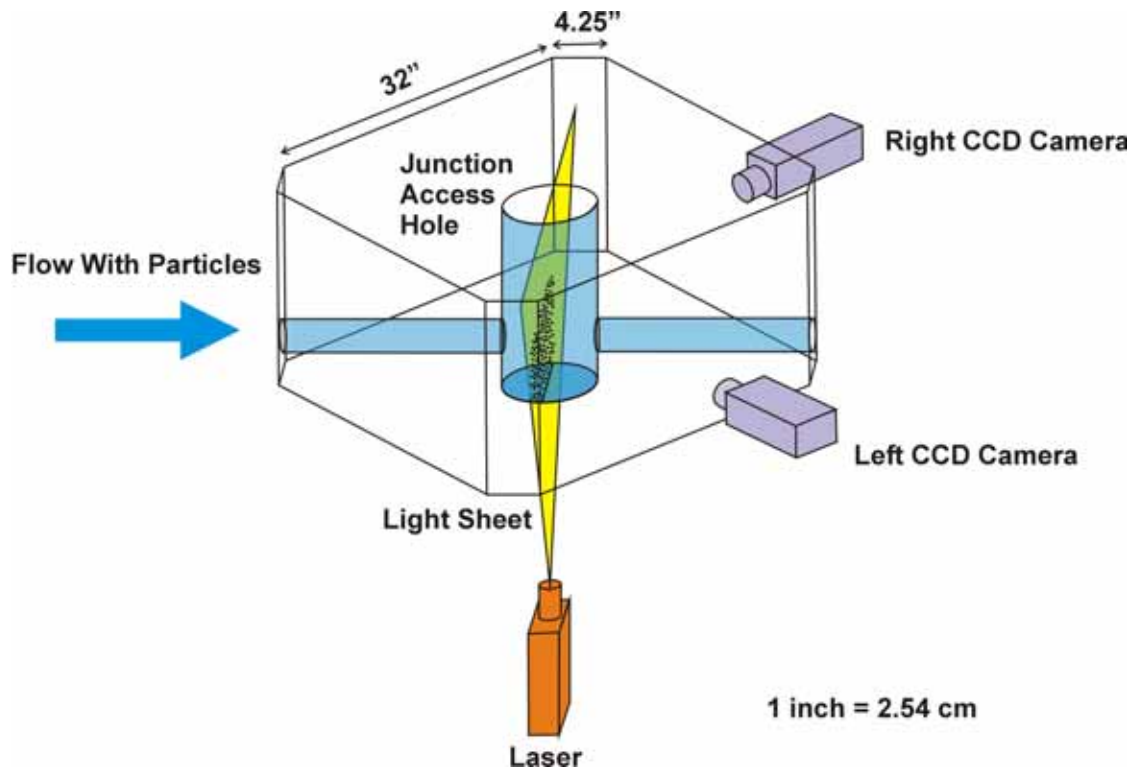
Figure 7. Diagram. Stereoscopic PIV arrangement and the access hole setup.
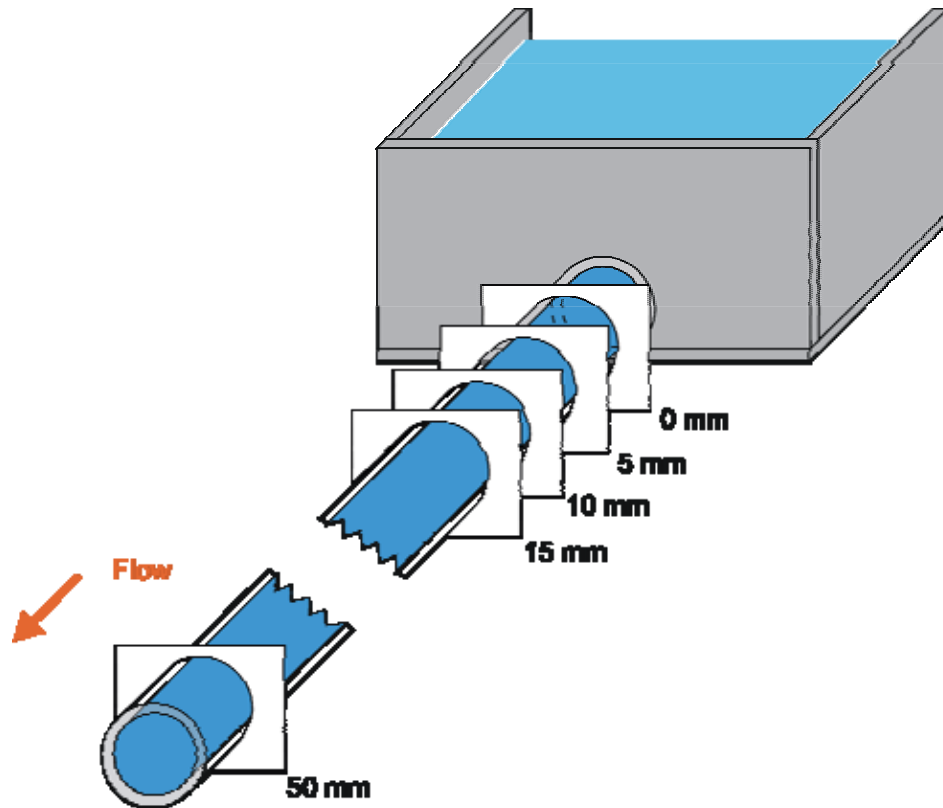
Figure 8. Diagram. Eleven stereoscopic PIV measurements along the miniculvert outflow pipe.

The stereoscopic PIV camera system consists of a pair of digital cameras that focus on two different angles of the vertically projected "light sheet" (see figures 9 and 10). The light sheet is generated with a laser fitted with an optical lens that spreads the beam into a plane of light. A special geometry is necessary to reconstruct the 3–D field from the two projected, planar displacement fields. This setup requires precise measurements of the distance between the two camera lenses, and the distances between each camera and the light sheet. The laser system and cameras are mounted on a movable carriage frame that keeps the distance constant between cameras and light sheet. It should also be noted that the CIS measurements and PIV measurements could not be measured at the same time, which resulted in running many of the experiments twice.
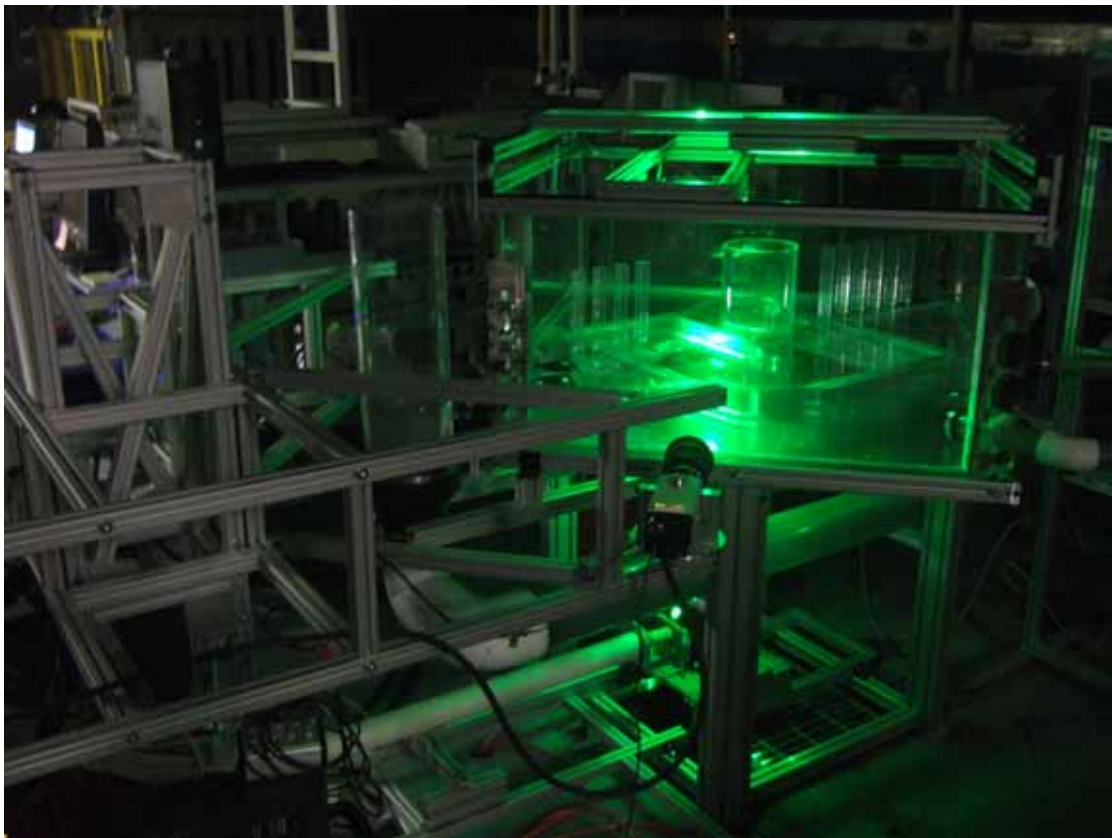
Figure 9. Photo. Access hole setup with PIV light sheet in outflow pipe.
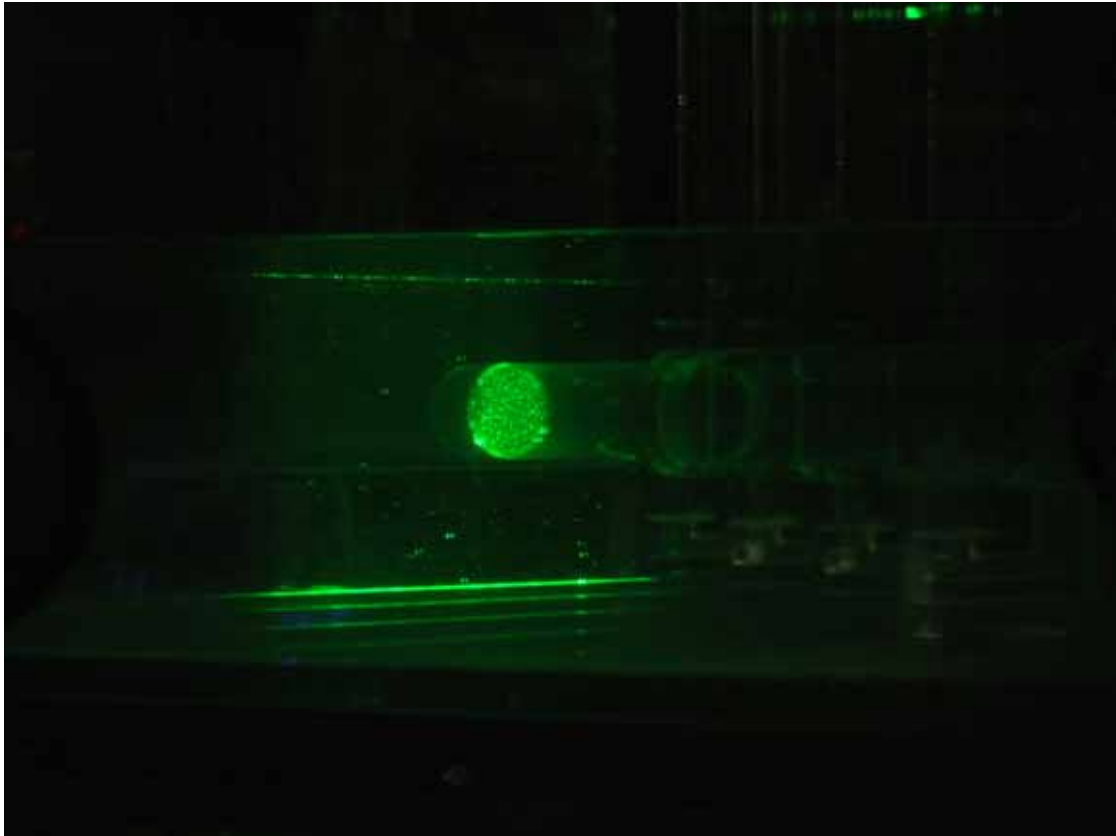
**Figure 10. Photo. Closeup of the tracer particles in the outflow pipe
from the access hole.**

4. RESULTS

SCALING EFFECTS

The first set of tests was designed to verify the effect of scale on the access hole (junction) loss experiments. A subset of the base runs (one inflow and one outflow pipe) was used to analyze scaling issues. The dimensions of the apparatus for the base runs were scaled down by a scaling ratio factor of 1 to 4, and total energy loss across the access hole was measured. Figure 11 shows that scaling had little effect on relative energy loss; that is, a change in dimensions was matched by a proportionate change in energy loss.

Figure with $\Delta E_{old} = 0.8819 * \Delta E_{new}$ and $R^2 = 0.9344$. Y-axis: Total Energy Loss (mm) in old model scale. X-axis: Total Enery Loss (mm) in new model scale.
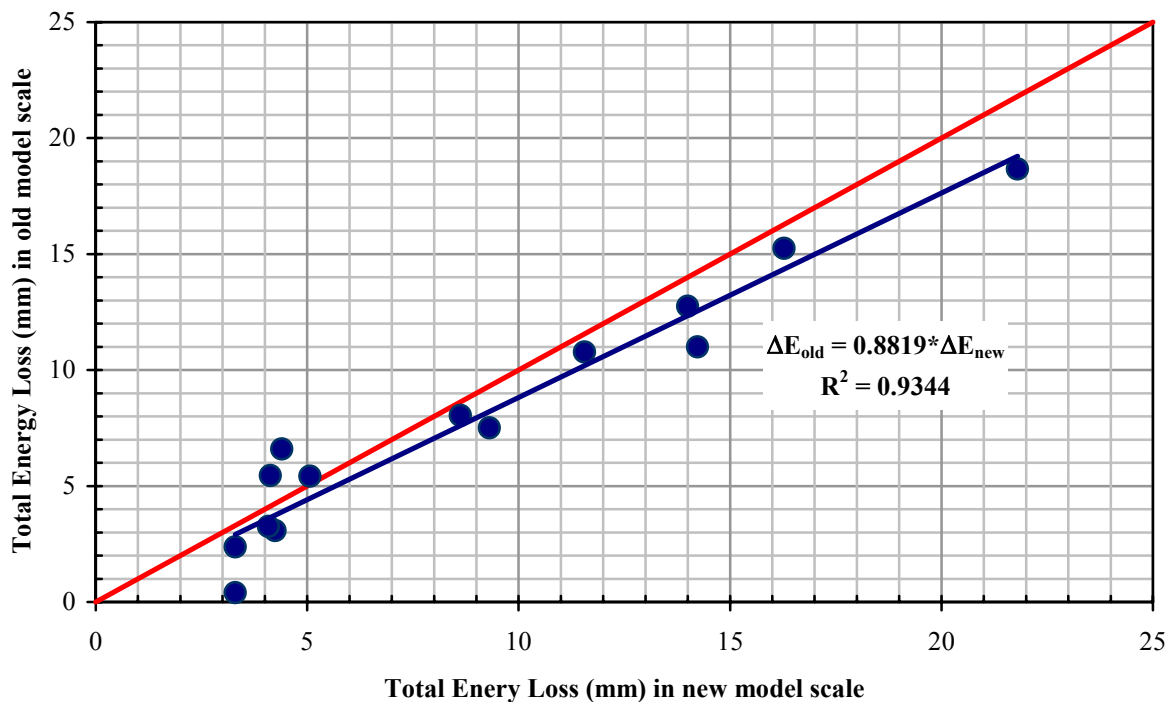
Figure 11. Graph. Effects of scaling.

VALIDATION OF K_i AND K_o

The next set of tests was designed to validate the loss coefficients for the inflow pipe (an exit loss) and the outflow pipe (an entrance loss). The first idea for calculating these losses involved measuring the kinetic energy distribution across the access hole. This idea, however, did not work well because the flow in the access hole was too turbulent and chaotic to characterize. The final idea was to measure the outflow energy loss and then infer the inflow energy loss using two basic steps.

The first step was to design a miniculvert apparatus with scaled conditions similar to the access hole apparatus. The miniculvert apparatus was used to isolate the entrance loss for the outlet pipe by measuring the velocity along the outflow pipe (using PIV) and the HGL (using standpipes and

CIS) along the outflow pipe and in the headbox of the miniculvert apparatus. The EGL was calculated by summing the measured HGL and the velocity head. The difference in the EGLs projected to the headwall yielded the energy loss in the outflow pipe (a contraction entrance loss). The main idea of the first step was then to determine if there is a direct correlation between the measured energy loss and the area of maximum contraction in the outflow pipe, often referred to as the vena contracta, as suggested by Morris.[8] Conceptually, the vena contracta is a reduced flow area that conveys most of the through-flow downstream of a contraction. In reality, though, with experimental measurements, the area and the location of the vena contracta is not readily apparent, and the area is highly subjective. The location was determined by taking velocity measurements at several sections, as illustrated in figure 8, to determine where the maximum local velocities occur. Researchers tried several techniques for defining the contracted area and ultimately selected a repeatable technique that measures the area containing a prescribed percentage of the maximum velocities in each cross section.

Figure 12 is an example of a shaded contour plot of the velocity profile at a location along the outflow pipe. The lightest shade of gray in this figure represents all of the velocities that are less than 86.6 percent of the highest velocity in the profile. The three contours near the center, in order from light to dark, represent the velocities greater than 86.6, 90.0, and 92.5 percent of the maximum velocity in the cross section, respectively. Appendix A has an example of the velocity profile at each location along the outflow pipe.
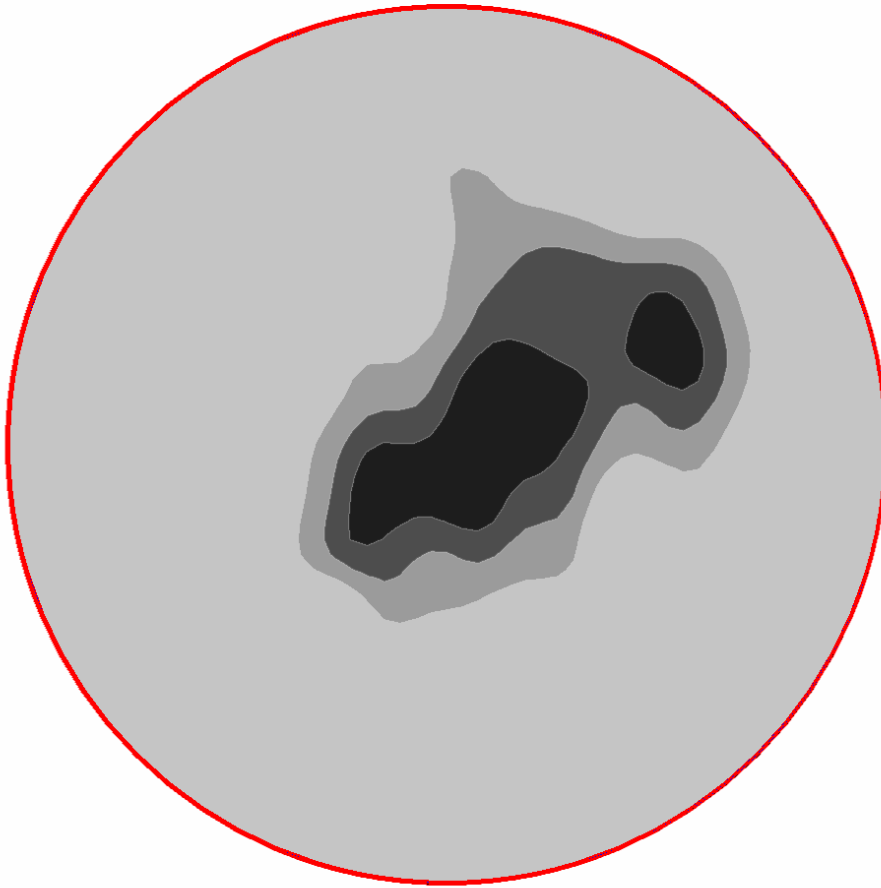
Figure 12. Image. Selected contours of velocity magnitude in the outflow pipe.

Now consider the following definitions.

A_o is the cross-sectional area of the outlet pipe (m^2).

A_k is the cross-sectional area associated with a contour of velocity (m^2).

K is the subscript denoting a contour of velocity where V is greater than 86.6, 90, or 92.5 percent.

ΔE_{oc} is the energy loss in the outflow pipe (a contraction entrance loss (m)).

D_o is the diameter of the outlet pipe (m).

The relative area, A_k over A_o, enclosed by these three contours was then correlated with the ratio of the outflow energy loss, ΔE_{oc}, over the diameter of the pipe, D_o (equation 17).

$$\frac{\Delta E_{oc}}{D_o} = f\left(\frac{A_k}{A_o}\right) \tag{17}$$

Table 2 shows the distance along the outflow pipe from the culvert (see figure 8) where A_k was used in the calibration, which again was selected based on where the integrated velocity was the

largest (i.e., the point closest to the maximum contraction in the pipe). Appendix B shows the contours of maximum velocity that were measured at these locations in each miniculvert run.

Table 2. Distance along the culvert outflow pipe where A_k was measured.

A_k Measured	Miniculvert Experiment		
	$Q/A_o = 42$ cm/s	$Q/A_o = 57$ cm/s	$Q/A_o = 69$ cm/s
$A_{86.6}$	0 mm	5 mm	0 mm
A_{90}	0 mm	5 mm	0 mm
$A_{92.5}$	0 mm	5 mm	0 mm

Figures 13 to 15 show that there is a strong correlation between the contraction energy loss and the contracted-area ratio regardless of which velocity contour was selected for the contracted area. The regression equations shown in figures 13 to 15 can be used to estimate the entrance energy loss for the outlet pipes in the access hole experiments (i.e., using measurements of these areas of maximum velocity).
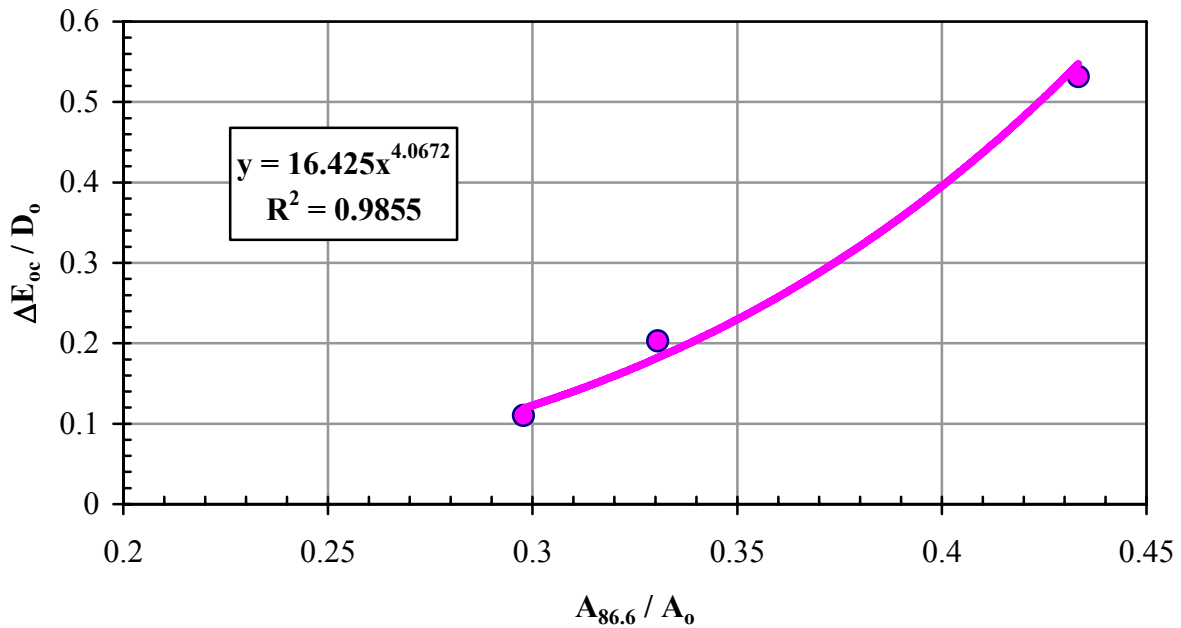
Figure 13. Graph. Correlation of ΔE_{oc} and $A_{86.6}$.
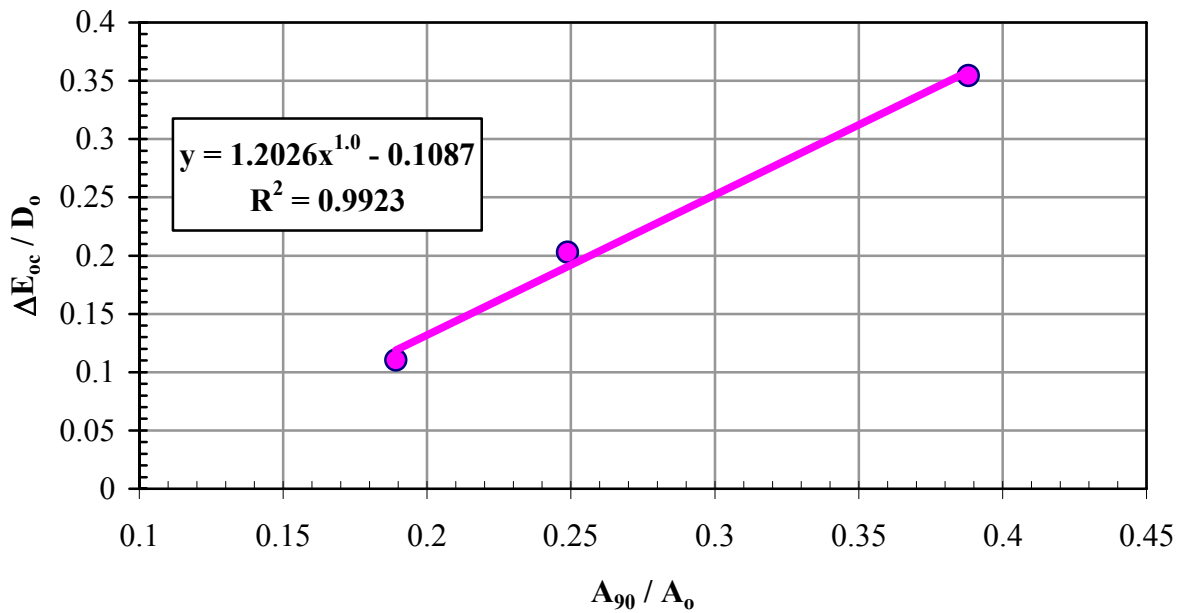
Figure 14. Graph. Correlation of ΔE_{oc} and A_{90}.

The graph shows:
$$y = 1.2026x^{1.0} - 0.1087$$
$$R^2 = 0.9923$$

with x-axis labeled A_{90} / A_o and y-axis labeled $\Delta E_{oc} / D_o$.
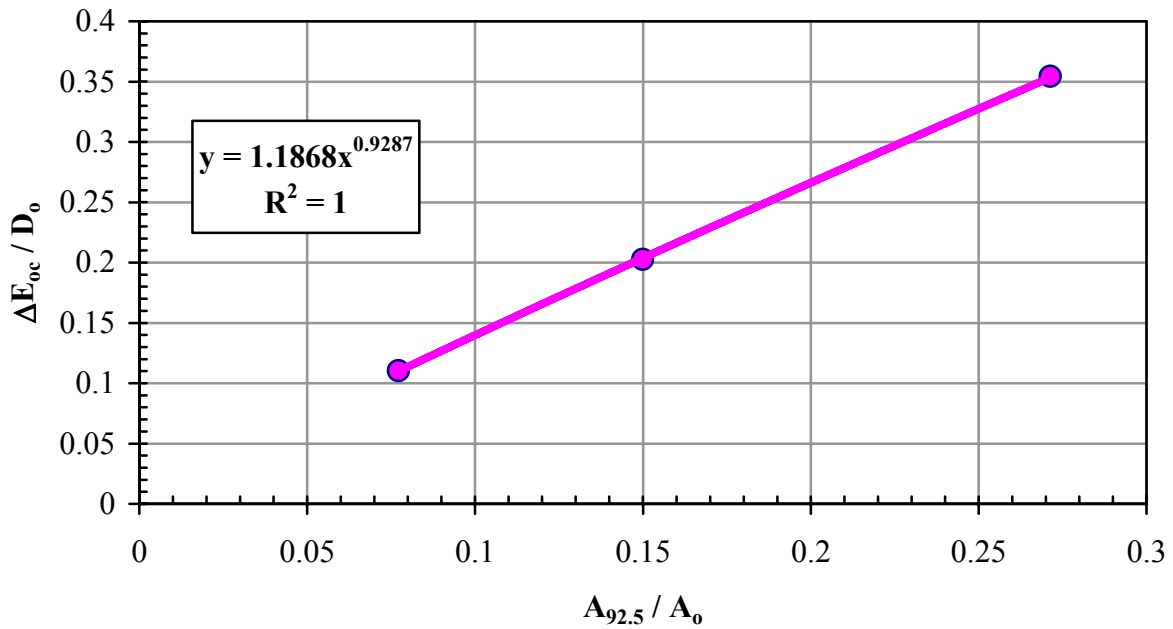
Figure 15. Graph. Correlation of ΔE_{oc} and $A_{92.5}$.

The graph shows:
$$y = 1.1868x^{0.9287}$$
$$R^2 = 1$$

with x-axis labeled $A_{92.5} / A_o$ and y-axis labeled $\Delta E_{oc} / D_o$.

The second step in validating the inflow and outflow pipe loss coefficients used the access hole setup to run experiments with scaled conditions similar to four of the original junction loss experiments—labeled JCT114 through JCT117 in Appendix B of the report by Chang et al.[1] When these experiments were rerun using the scaled model, the HGL was measured using

standpipes and CIS, and velocity profiles were measured using PIV. The total energy loss across the access hole was measured by summing the measured HGL and the velocity head. Table 3 shows the total energy loss across the access hole in each experiment.

Table 3. Total energy loss across the access hole.

Q/A_o = 43 cm/s	Q/A_o = 57 cm/s	Q/A_o = 64 cm/s	Q/A_o = 75 cm/s
4.1 mm	9.3 mm	14.2 mm	16.3 mm

Similarly, table 4 shows the distance along the outflow pipe (from the access hole) where the maximum contraction and A_k were measured. Appendix C shows contours of maximum velocity that were measured at these locations in each access hole run.

Table 4. Distance along the access hole outflow pipe where A_k was measured.

	Access Hole Experiment			
A_k Measured	Q/A_o = 43 cm/s	Q/A_o = 57 cm/s	Q/A_o = 64 cm/s	Q/A_o = 75 cm/s
$A_{86.6}$	5 mm	0 mm	0 mm	0 mm
A_{90}	5 mm	0 mm	0 mm	0 mm
$A_{92.5}$	5 mm	0 mm	0 mm	0 mm

The energy loss in the outflow pipe (an entrance loss) was then computed using the measured area of maximum velocity and the relationships from figures 13 to 15. Figure 16 shows that the relationship between the computed outflow energy loss and the velocity head is fairly strong. Recalling equation 4, the slope of the line in this figure shows that the outflow (entrance) loss coefficient, K_o, is approximately 0.16, which is remarkably close to Kilgore's estimate of 0.2.
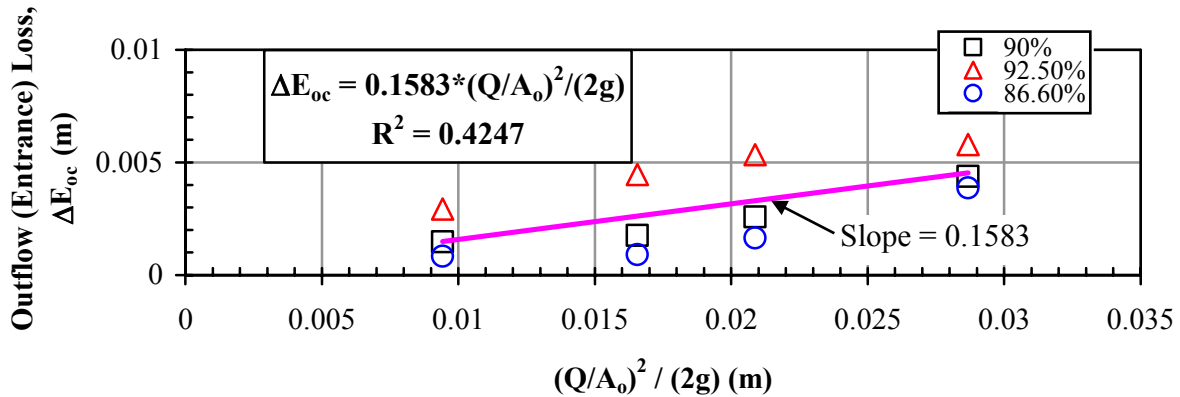
Figure 16. Graph. Outflow (entrance) loss versus velocity head.

The inflow (exit) loss (ΔE_i) was then calculated from the total energy loss (ΔE_{total}) and the outflow (entrance) loss (ΔE_{oc}) (equation 18).

$$\Delta E_i = \Delta E_{total} - \Delta E_{oc} \tag{18}$$

Figure 17 shows that the relationship between the computed inflow energy loss and the inflow velocity head is strong. Recalling equation 16, the slope of the line in this figure shows that the inflow (exit) loss coefficient, K_i, is approximately 0.43, which is very close to Kilgore's estimate of 0.4.
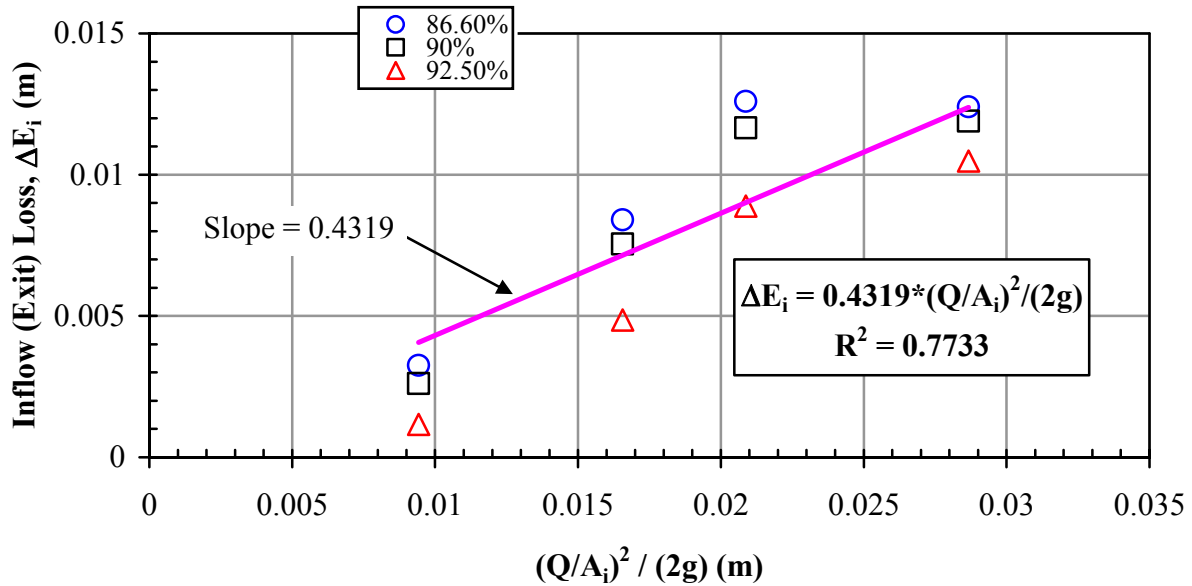
Figure 17. Graph. Inflow (exit) loss versus velocity head.

BASE RUNS

Next in the current lab study, 15 runs in the access hole setup were conducted to test the total energy loss predicted by the new junction loss method. These experiments all had a level outflow pipe, and an inflow pipe oriented at 180°. Table 5 shows the discharge intensities and access hole depths that were maintained in each run. The measured total energy loss across the access hole was then plotted versus the discharge intensity and compared to the total energy predicted by the new junction loss method using K_i equal to 0.43 and K_o equal to 0.16. Figure 18 shows that the new method matches the new lab data very well.

Table 5. Parameters for the 15 base runs.

Run	D_I	Average Access Hole Depth (cm)
1	0.71	4
2	0.94	4.45
3	1.05	7.02
4	1.22	10.02
5	1.22	11.05
6	1.03	6.4
7	0.23	7.46
8	0.44	7.51
9	0.44	11.08
10	0.66	5.6
11	0.66	11.01
12	0.89	9.61
13	0.67	7.45
14	0.67	11.2
15	1.09	7.7
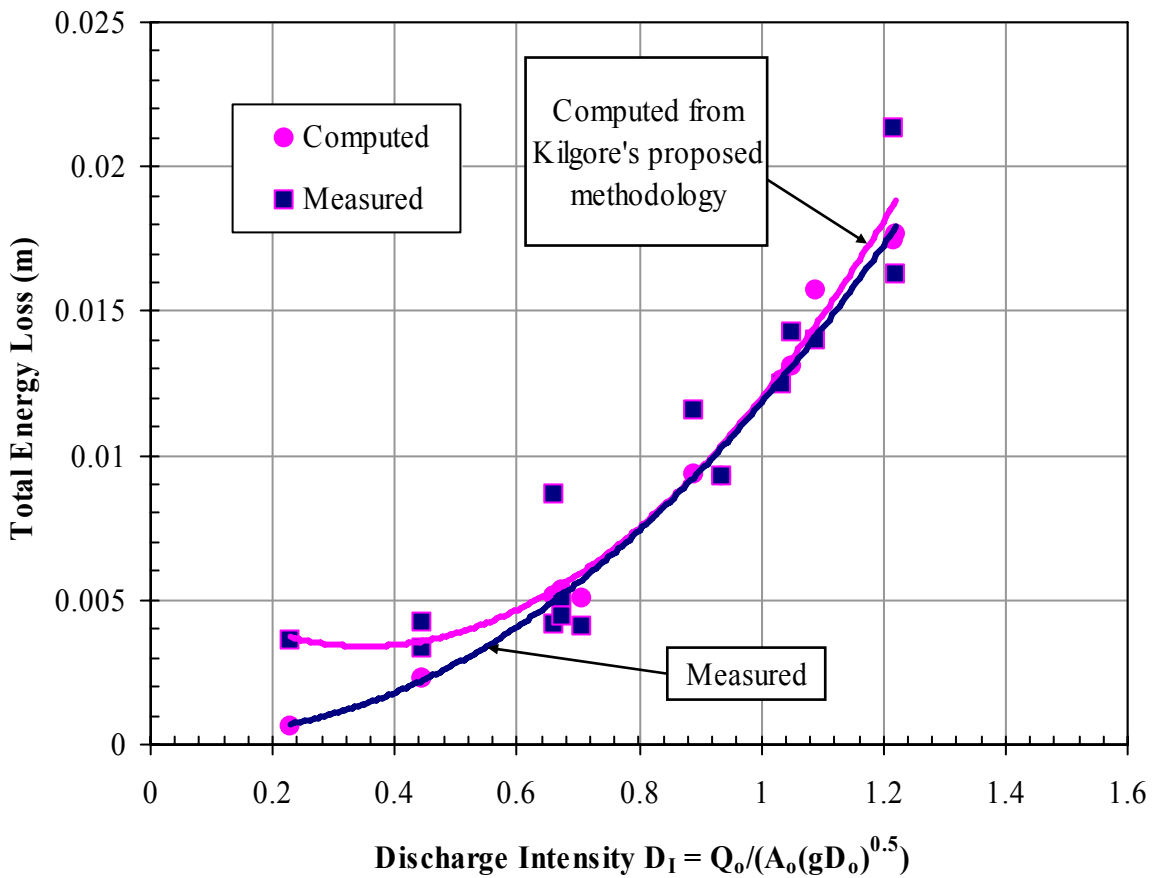
Figure 18. Graph. Validation of total energy loss calculations.

26

SUPERCRITICAL OUTFLOW AND ANGLED INFLOW

One of the major limitations of the existing FHWA methodologies is a failure to apply to some steep terrain conditions. The proposed new procedure addresses the problem with steep outflow pipes by defaulting to inlet control equations 7 and 8 to compute the base flow depth in the access hole. Eighteen runs were conducted with supercritical flow in the outflow pipe as part of this lab study to test the applicability of the proposed procedure for steep pipes. These experiments also included three different inflow pipe configurations (i.e., angled inflow). Supercritical flow was assured by using a 3 percent slope for the outflow pipe. Recall also that K_i equals 0.43, and K_o equals 0.16. One surprising result of these tests was an almost constant depth in the center of the access hole for a fairly wide range of discharge intensities. Figures 19 to 21 generally show that the new junction loss methodology does a good job of estimating the EGL elevations in the inflow pipes for supercritical flow situations. The only exception, which Kilgore anticipated, appears to be when one inflow pipe is oriented at 180° with high discharge intensity into a supercritical outflow pipe. Kilgore anticipated that water shooting directly across an access hole in a jet into a supercritical outflow pipe may not expand and contract again in the way that this method predicts.
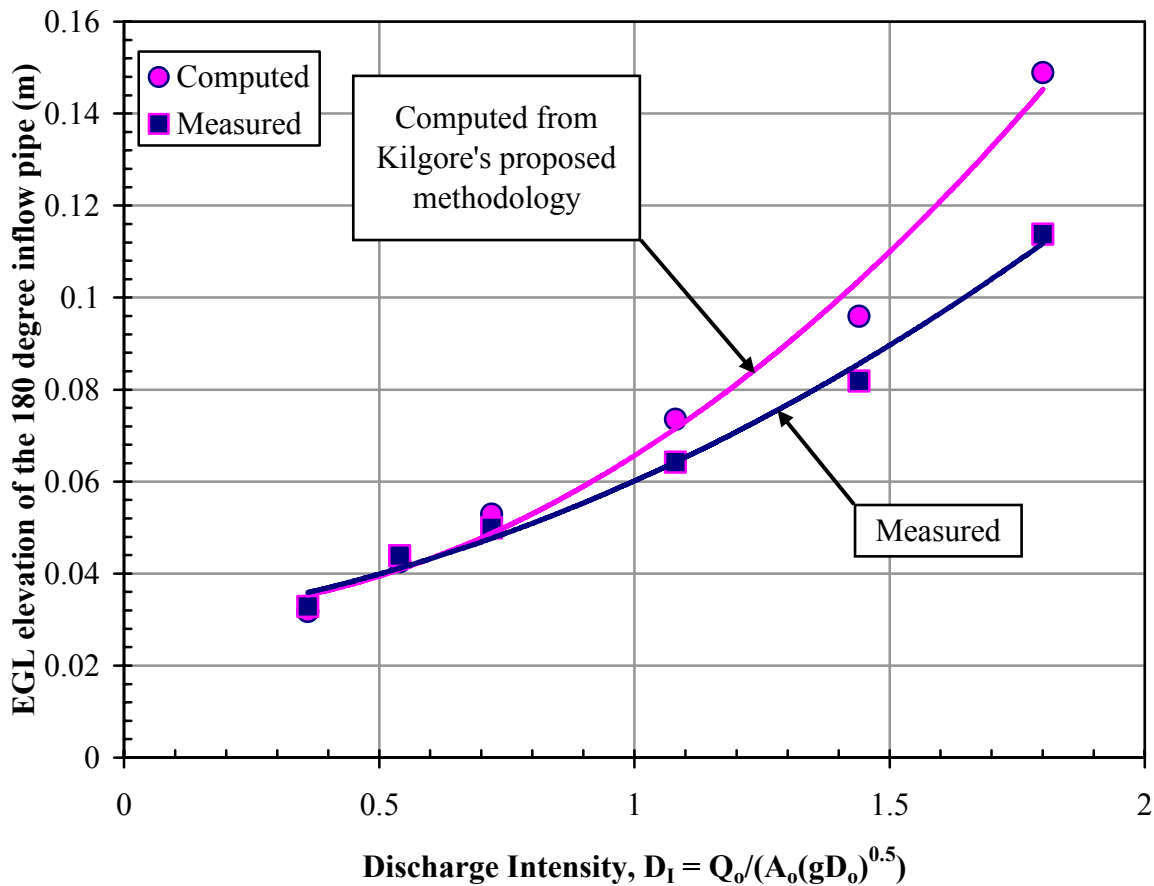
Figure 19. Graph. Validation of EGL with a 180° inflow pipe and supercritical outflow.
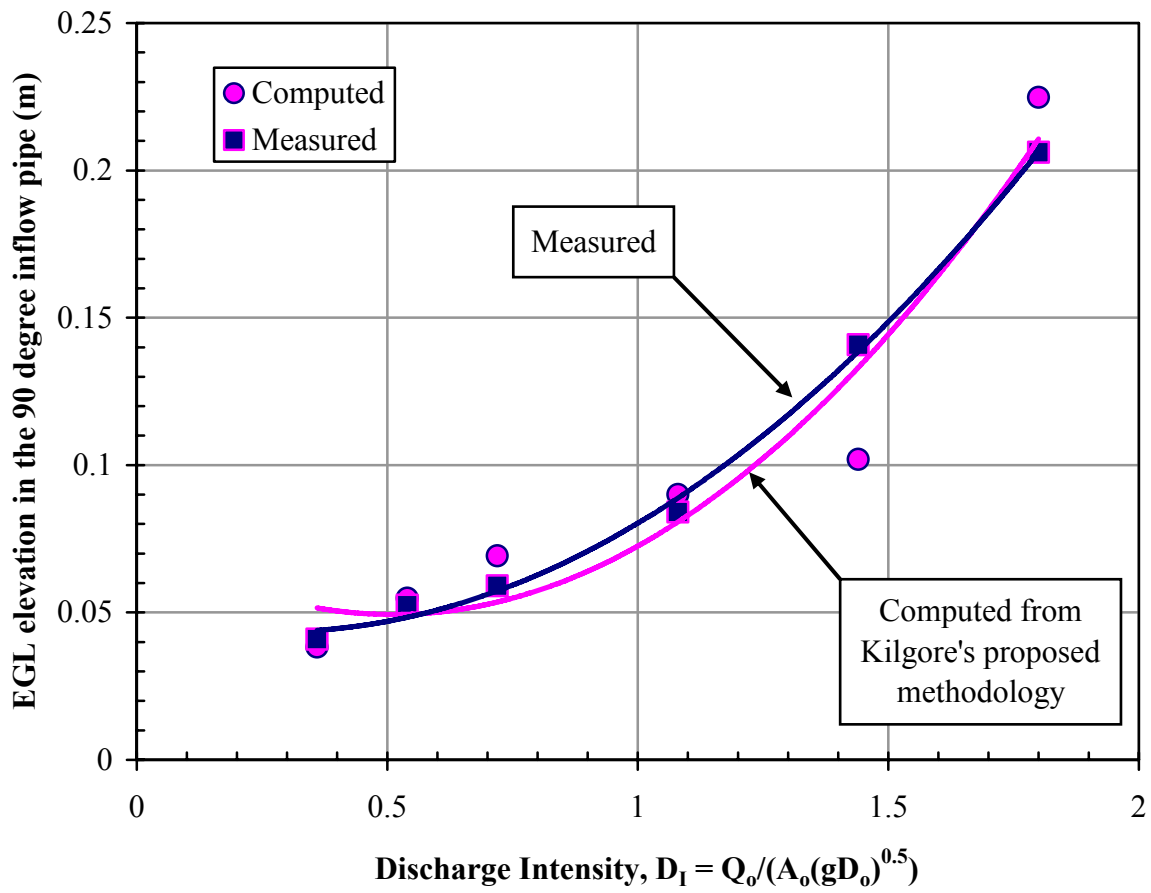
Figure 20. Graph. Validation of EGL with a 90° inflow pipe and supercritical outflow.

Axis labels and legend on the figure:

- Y-axis: EGL elevation in the 90 degree inflow pipe (m)
- X-axis: Discharge Intensity, $D_I = Q_o/(A_o(gD_o)^{0.5})$
- Legend: Computed, Measured
- Annotations: Measured; Computed from Kilgore's proposed methodology
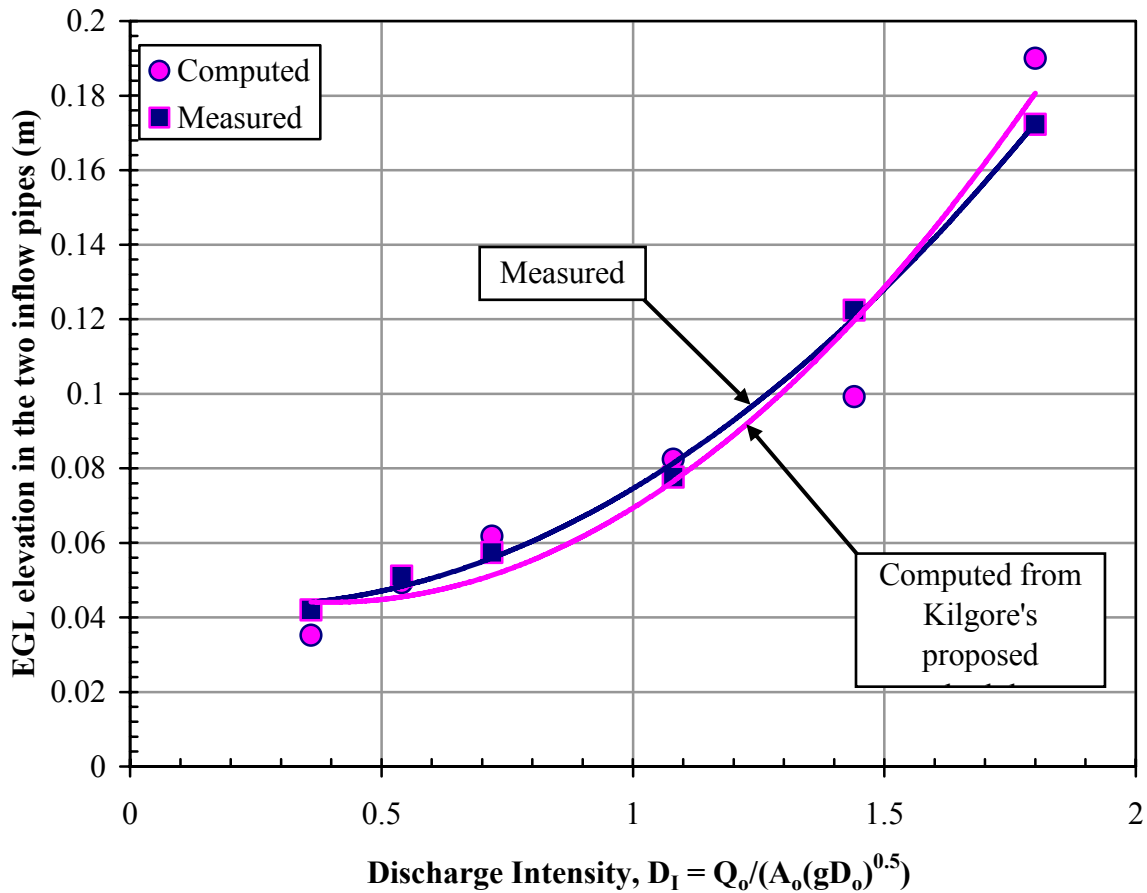
Figure 21. Graph. Validation of EGL with two inflow pipes and supercritical outflow.

PLUNGING INFLOW

The last runs 18 runs tested the method's prediction of energy loss with plunging inflow conditions. The drop in elevation for the inlet, with respect to the base of the outlet pipe, in these runs varied between 3 to 10 times the outflow pipe diameter, and two different access hole depths were maintained (i.e., $1.5D_o$ versus $3.0D_o$). Recall also that K_i equals 0.43, and K_o equals 0.16. Figure 22 shows that the new junction loss method predicts the EGL in the inflow pipe very well. This figure shows that the measured grade line is about 7 percent greater than what the existing junction loss method predicts.
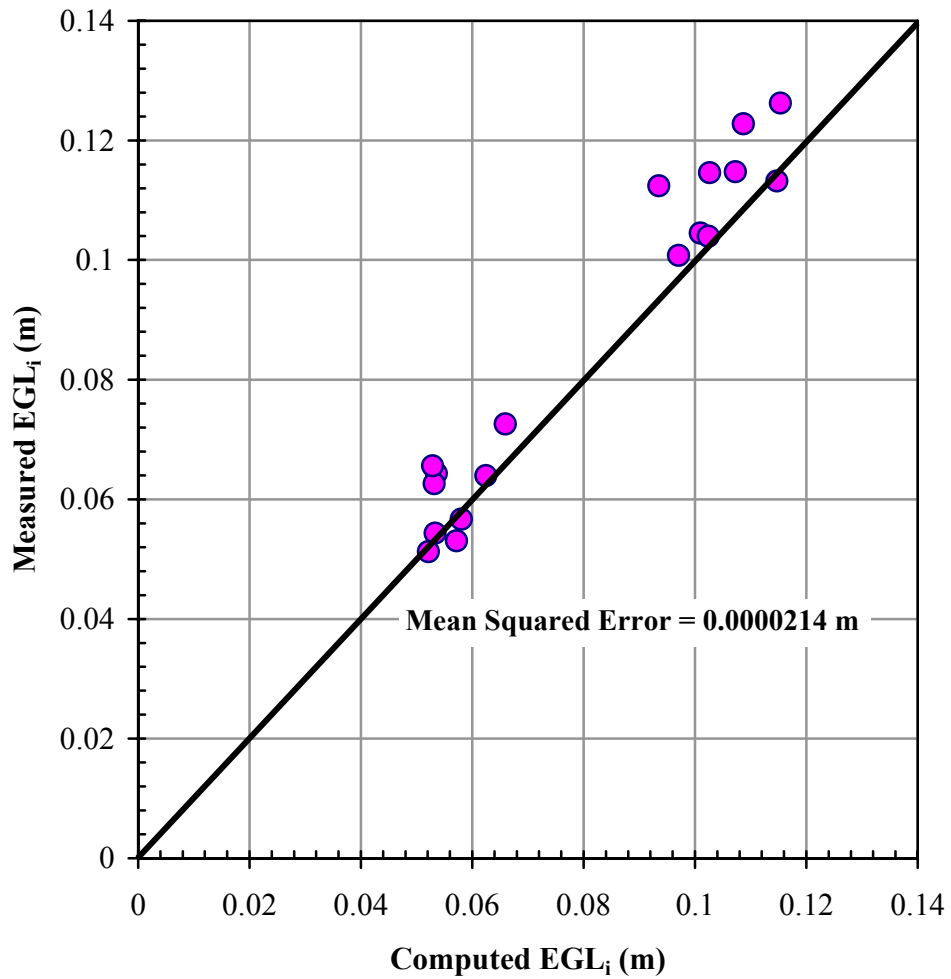
Figure 22. Graph. Validation of the total energy loss with plunging inflow.

Figures 23 and 24 show that the new junction loss method predicts the EGL in the nonplunging inflow pipe remarkably well over a variety of plunging inflow rates, plunging inlet elevations, and access hole water depths.
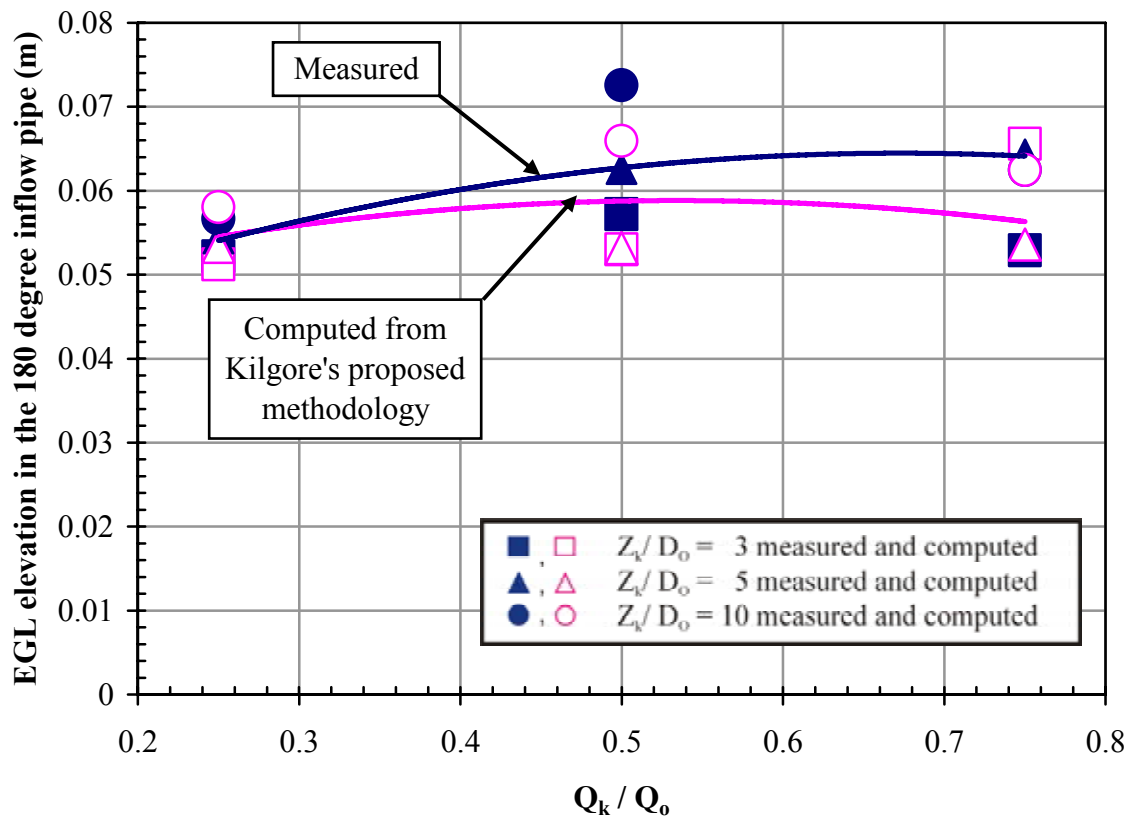
Figure 23. Graph. EGL in the inflow pipe versus plunging inflow rate for $E_a = 1.5D_o$.
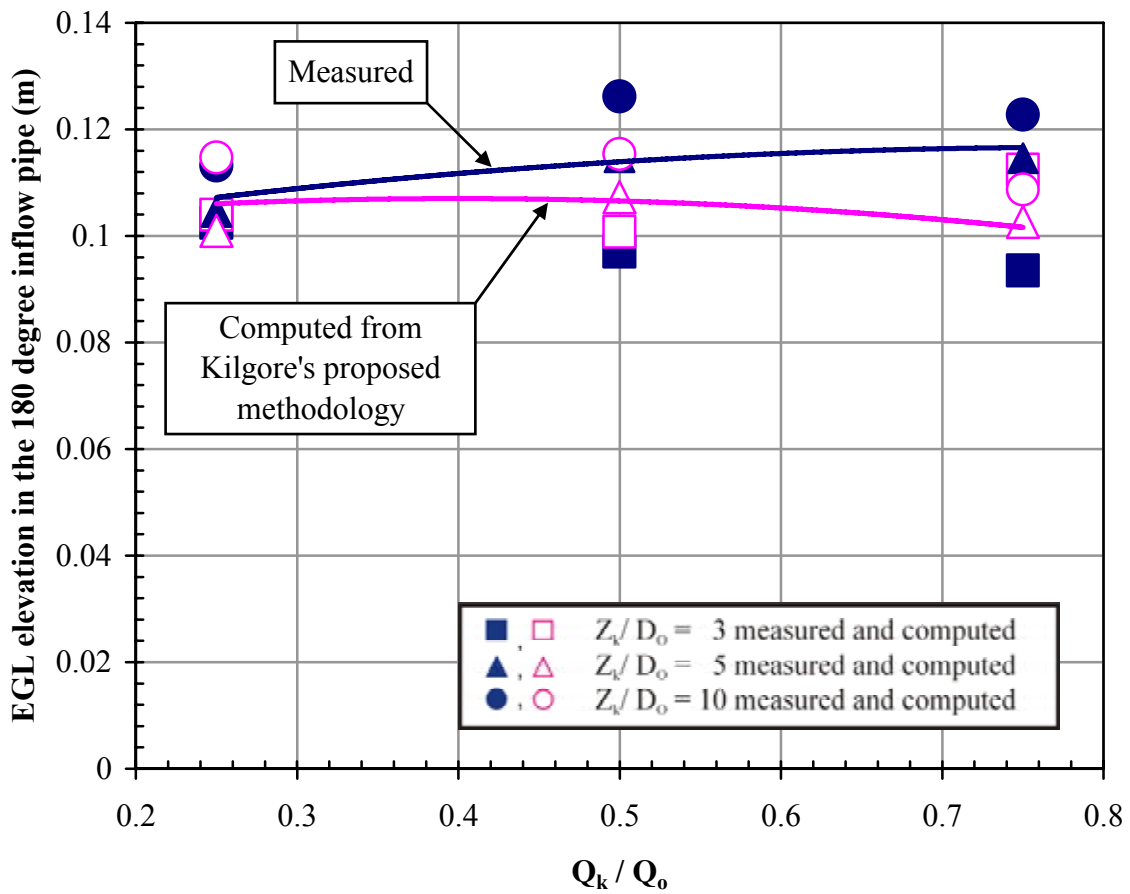
Figure 24. Graph. EGL in the inflow pipe versus plunging inflow rate for $E_a = 3.0D_o$.

5. CONCLUSIONS

One concern when conducting small-scale experiments is the scaling issue. Comparing the old base run data to the smaller scale base runs confirmed that small-scale models can be used with reasonable confidence to evaluate and develop the proposed junction loss method. Small-scale tests are much more efficient and reduce many of the physical and geometrical constraints. This is the primary reason why the experiments were able to determine that K_i equals 0.43, K_o equals 0.16, and the coefficient in equation 6 should be equal to 1.0 (i.e., equation 7). These values are remarkably close to Kilgore's values of 0.4 for K_i and 0.2 for K_o. The difference in values produces only minor differences in energy loss for pipe velocities less than 3.05 m/s (10 ft/s). It should also be noted that Kilgore's coefficients slightly overestimate the energy level in the access hole, which makes his coefficients slightly more conservative than the lab-determined values.

This new and revised methodology addresses the problem of supercritical flows in outflow pipes. The use of inlet controlled culvert equations to estimate the initial depth in the access hole for these situations appears to work very well. Kilgore proposed a relatively simple equation to compute additional energy loss for plunging flows that accounts for the proportion of the flow that is plunging and the drop height. The experiments show that the new junction loss method is applicable for plunge-height ratios (i.e., plunge height divided by outlet pipe diameter) up to 10.

Characterizing the kinetic energy in the access hole remains the most rational procedure for estimating energy losses in access holes and distributing those losses among several inflow pipes. The two approaches involving PIV and 3–D numerical modeling to analyze the energy level in the access hole, however, proved too difficult due to the extremely chaotic flow inside the access hole. This was the primary reason that the research focused on the more organized flow in the contracted area of the outflow pipe. The area of maximum velocity near the contraction zone was successfully used as an indirect measure of the energy loss in the outflow pipe (an entrance loss), which was then used to backcalculate the energy loss in the inflow pipe. This procedure showed that the entrance and exit losses predicted by the new junction loss method are remarkably accurate.

APPENDIX A. VELOCITY PROFILES AT 5 MM INCREMENTS

The following images show examples of the velocity profile in the outflow pipe from one of the miniculvert experiments. Blue indicates low velocity, while the spectrum toward red reflects increasing magnitudes of local velocity.
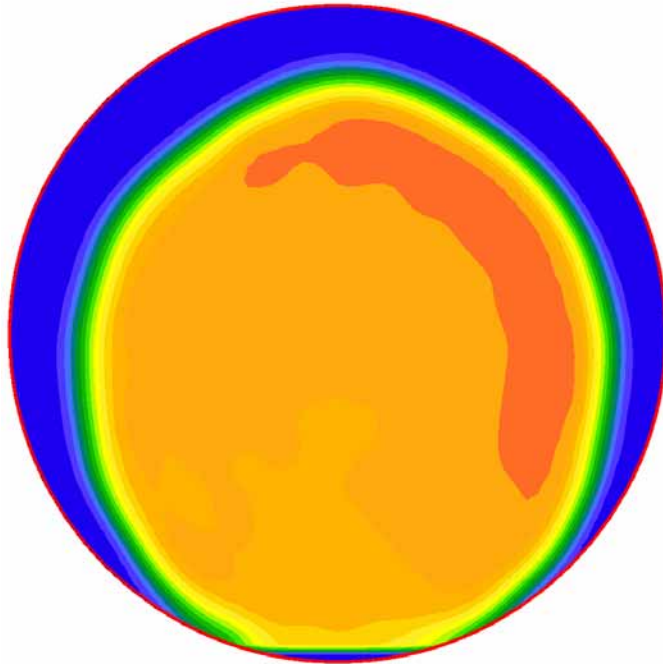
Figure 25. Image. Example velocity profile at the outlet.
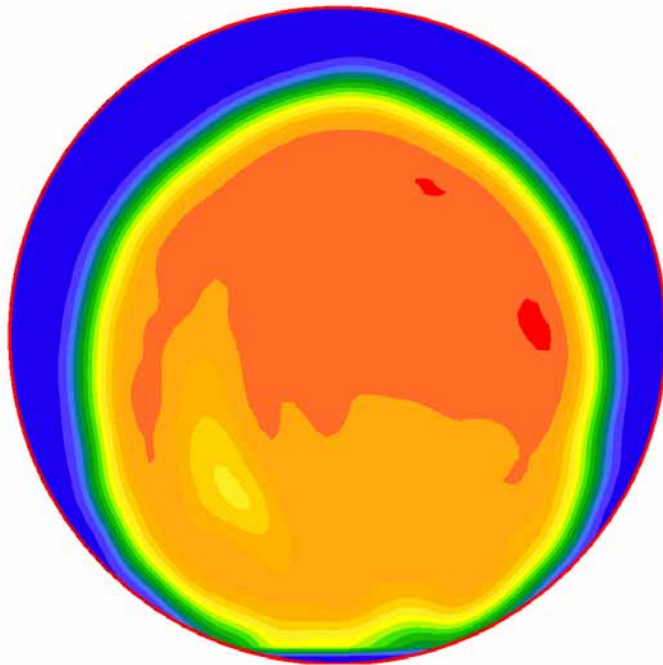
Figure 26. Image. Example velocity profile 5 mm (0.19 inch) from the outlet.
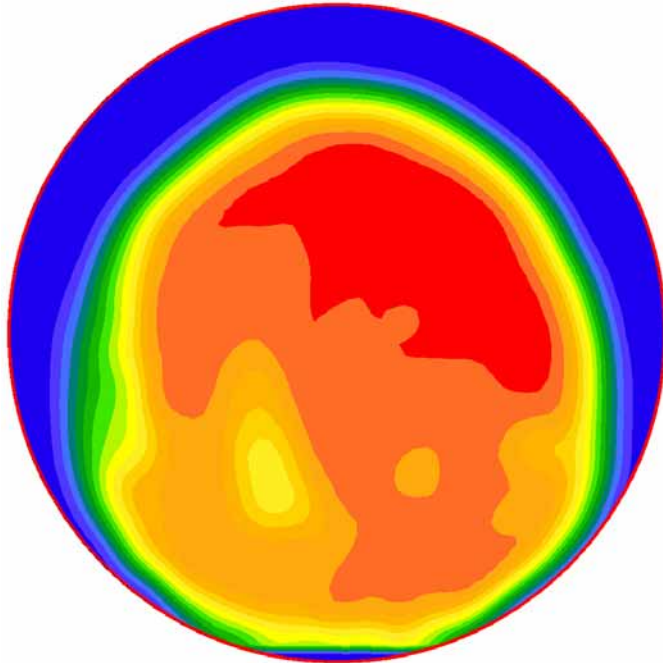
Figure 27. Image. Example velocity profile 10 mm (0.39 inch) from the outlet.
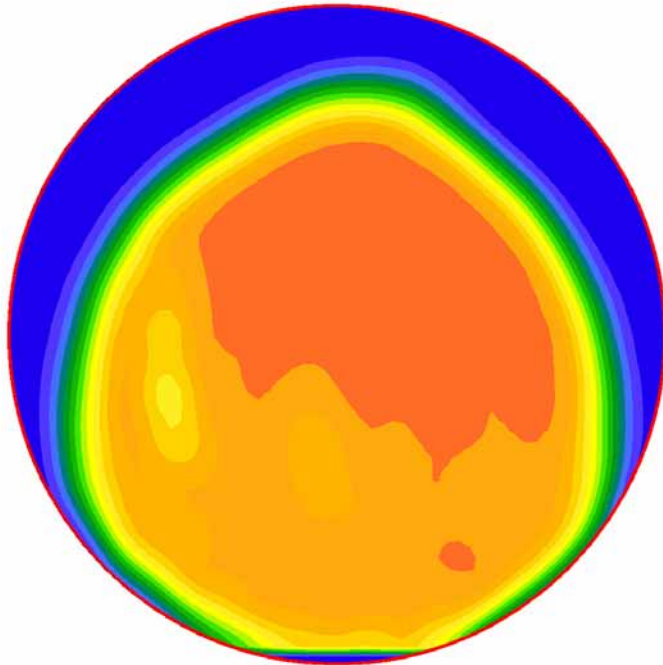
Figure 28. Image. Example velocity profile 15 mm (0.59 inch) from the outlet.
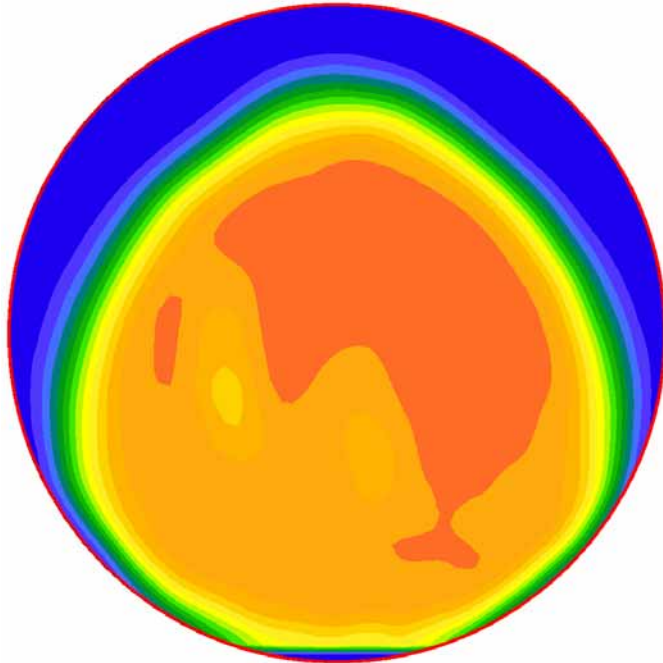
Figure 29. Image. Example velocity profile 20 mm (0.79 inch) from the outlet.
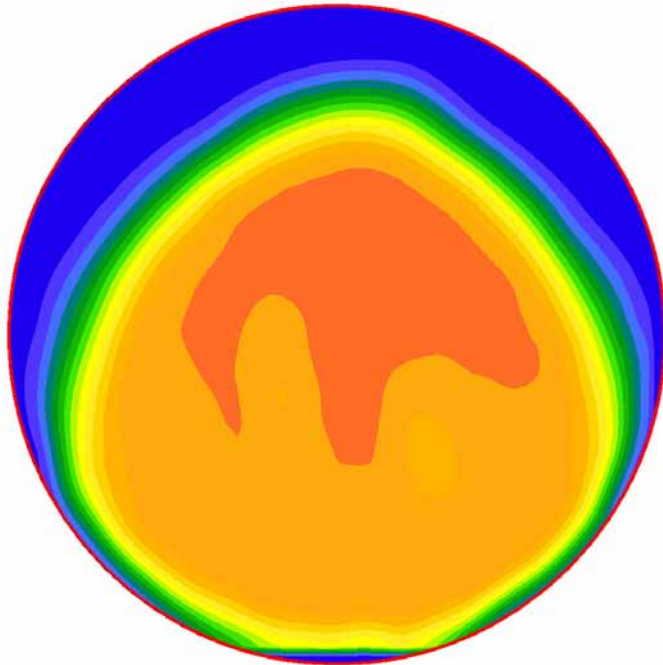
Figure 30. Image. Example velocity profile 25 mm (0.98 inch) from the outlet.
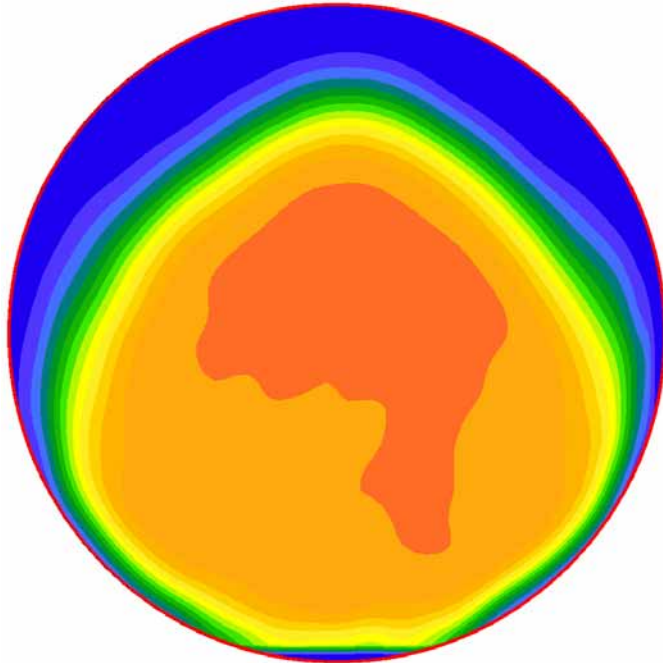
Figure 31. Image. Example velocity profile 30 mm (1.18 inches) from the outlet.
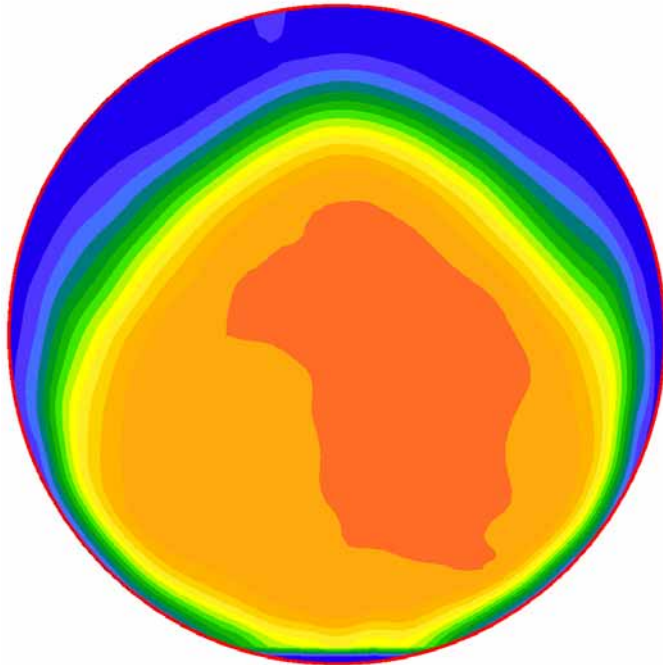
Figure 32. Image. Example velocity profile 35 mm (1.38 inches) from the outlet.
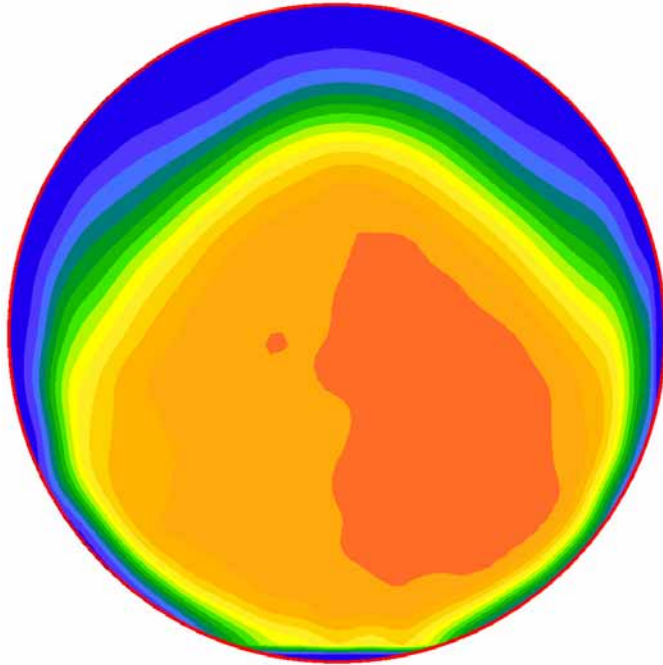
Figure 33. Image. Example velocity profile 40 mm (1.57 inches) from the outlet.
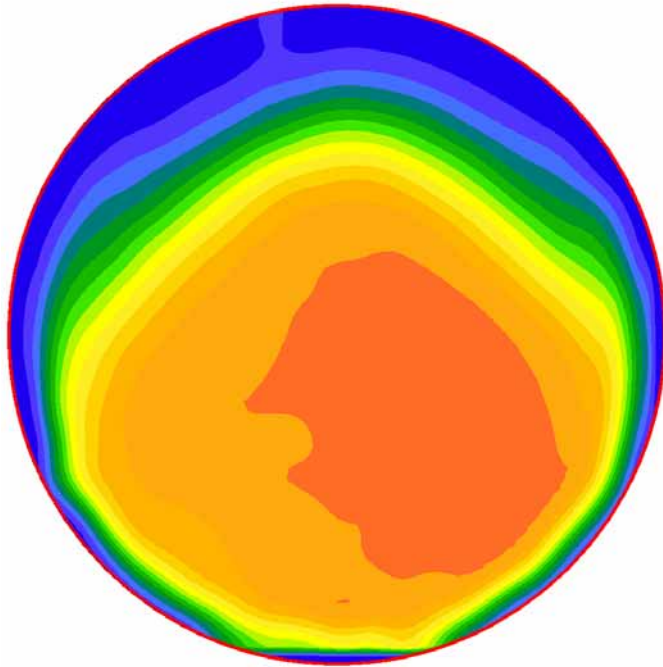
Figure 34. Image. Example velocity profile 45 mm (1.77 inches) from the outlet.
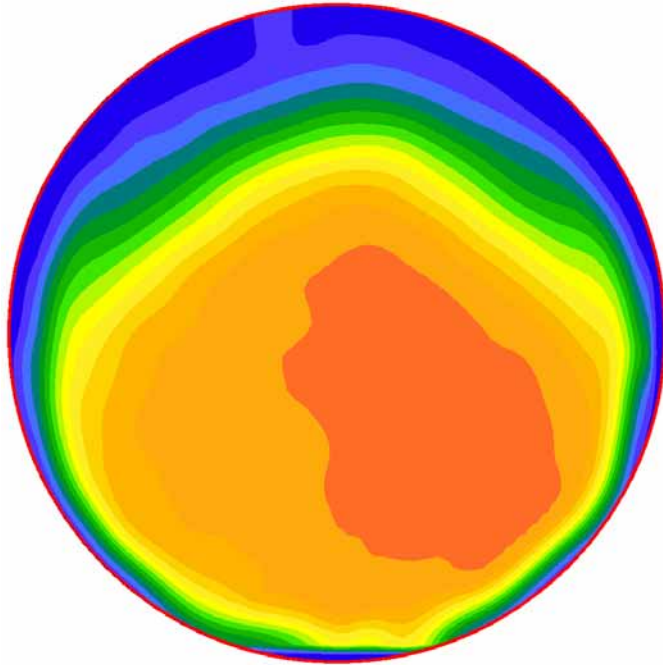
Figure 35. Image. Example velocity profile 50 mm (1.97 inches) from the outlet.

APPENDIX B. VELOCITY PROFILES USED IN THE MINICULVERT RUNS

The following images show the velocity profile in the outflow pipe from the miniculvert experiments. These were used to validate K_o. Blue indicates low velocity, while the spectrum toward red reflects increasing magnitudes of local velocity.
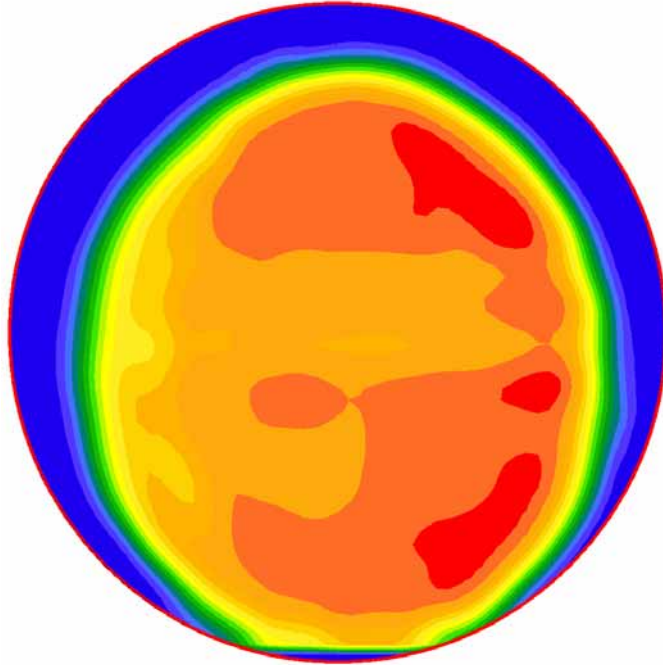
Figure 36. Image. Velocity profile at the outlet for Q/A_o = 42 cm/s (16 inches/s).
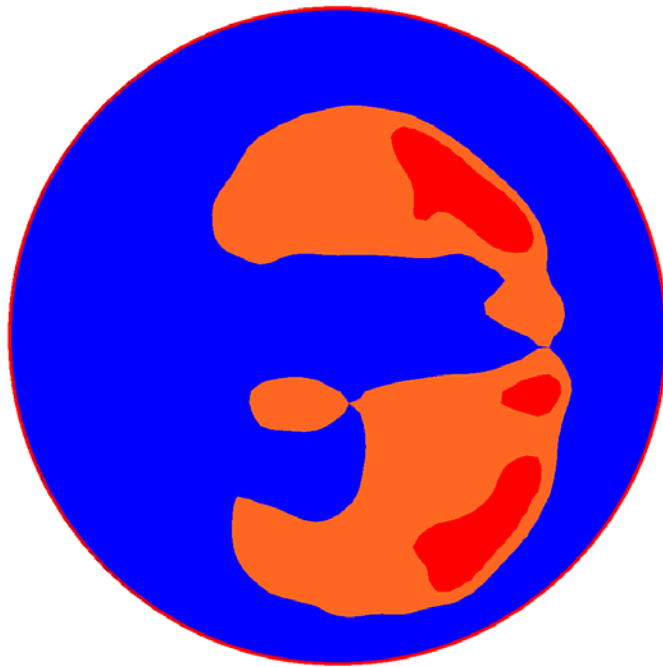
Figure 37. Image. Area where V is greater than $0.867V_{max}$ at the outlet for Q/A_o = 42 cm/s (16 inches/s).
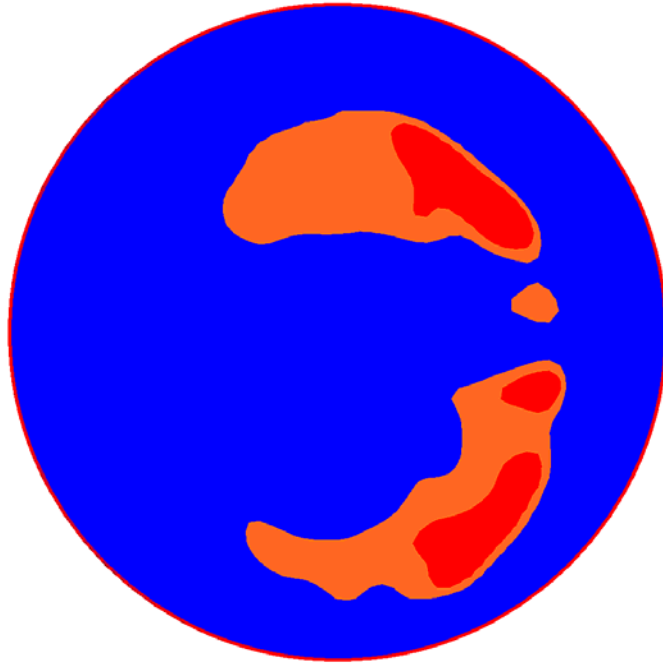
Figure 38. Image. Area where V is greater than 0.90V$_{max}$ at the outlet for Q/A$_o$ = 42 cm/s (16 inches/s).
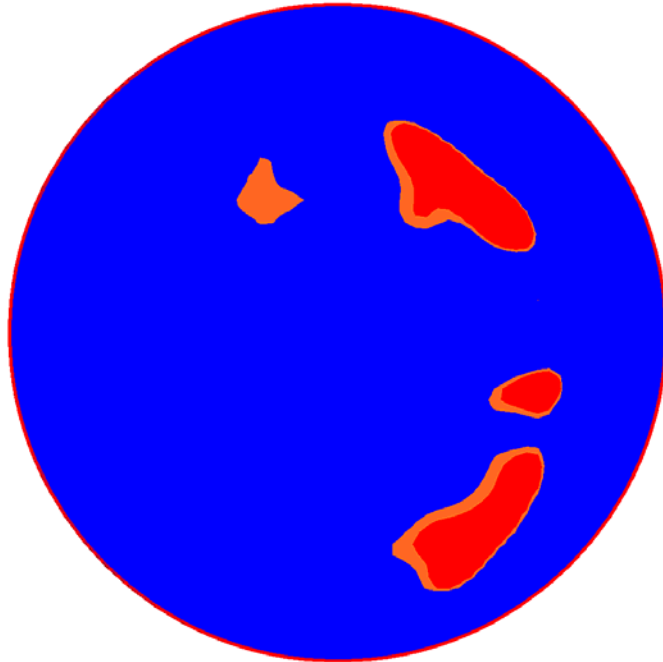
Figure 39. Image. Area where V is greater than 0.925V$_{max}$ at the outlet for (16 inches/s)Q/A$_o$ = 42 cm/s (16 inches/s).
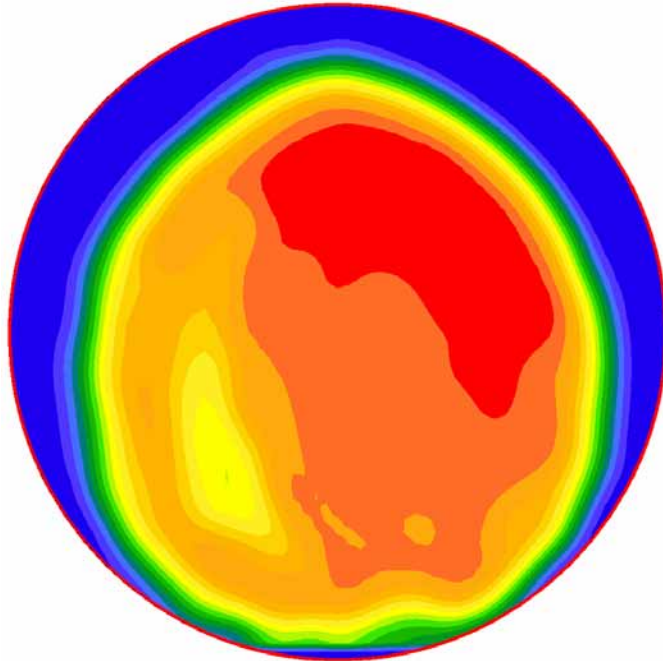
Figure 40. Image. Velocity profile 5mm (0.19 inch) from the outlet for Q/A_o = 57 cm/s (22 inches/s).
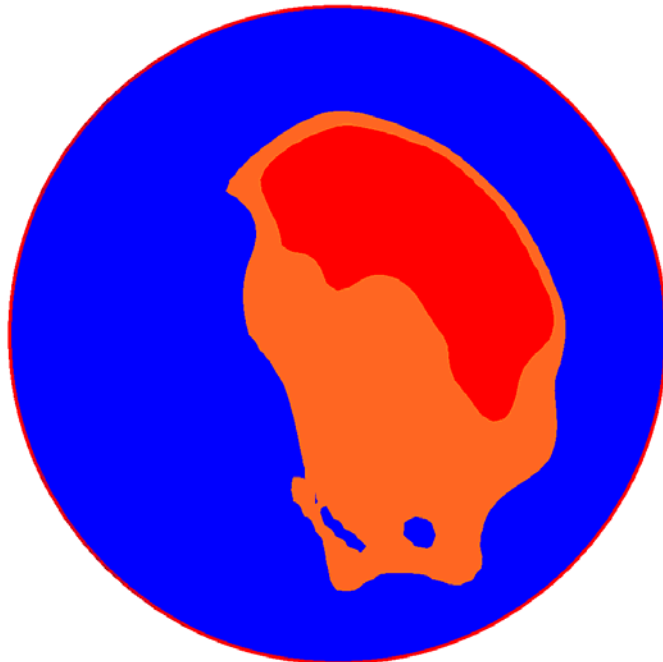
Figure 41. Image. Area where V is greater than $0.867V_{max}$ 5mm (0.19 inch) from the outlet for Q/A_o = 57 cm/s (22 inches/s).
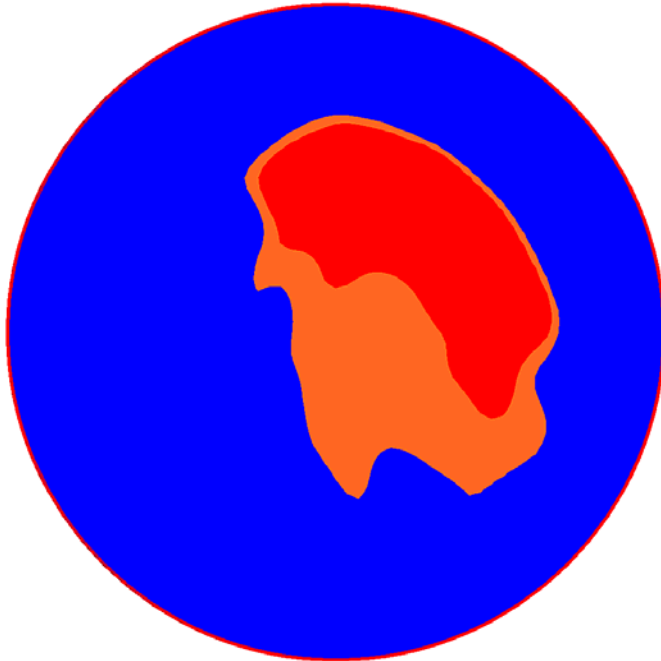
Figure 42. Image. Area where V is greater than $0.90V_{max}$ 5mm (0.19 inch) from the outlet for Q/A_o = 57 cm/s (22 inches/s).
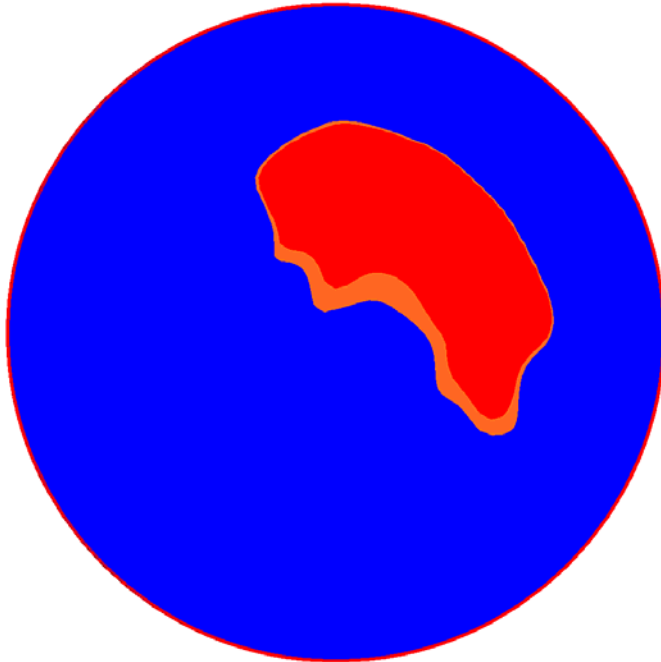
Figure 43. Image. Area where V is greater than $0.925V_{max}$ 5mm (0.19 inch) from the outlet for Q/A_o = 57 cm/s (22 inches/s).
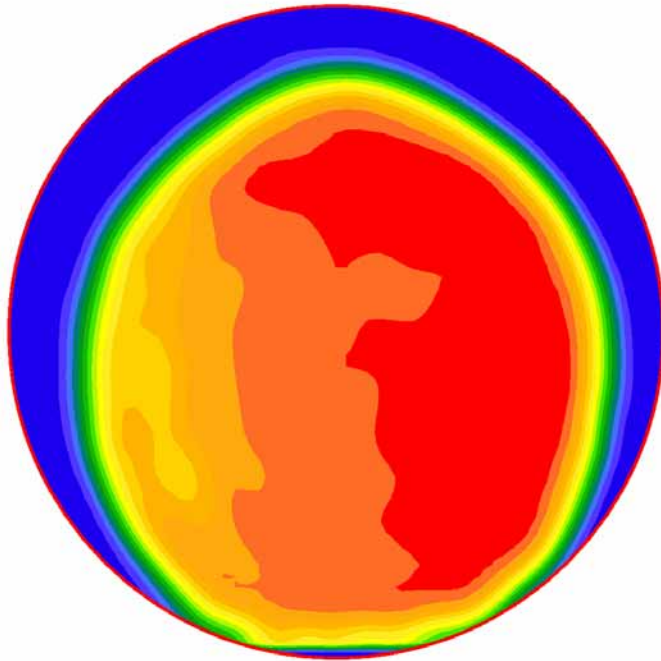
Figure 44. Image. Velocity profile at the outlet for $Q/A_o = 69$ cm/s (27 inches/s).
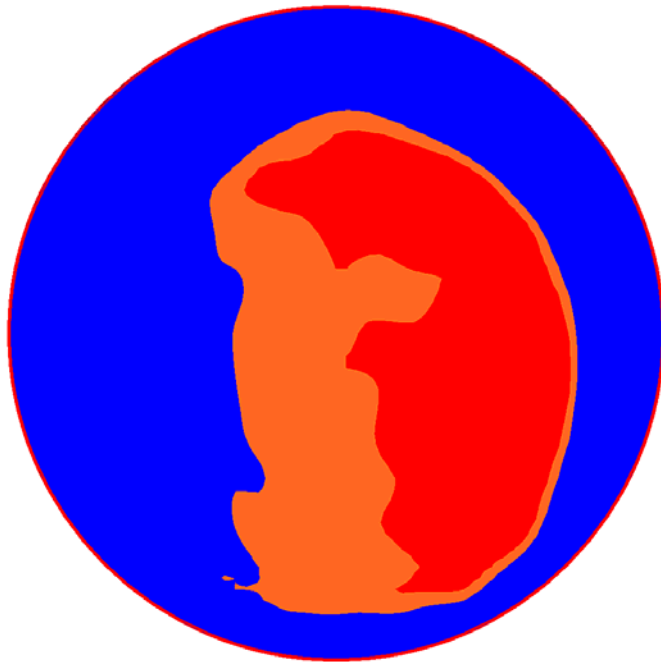
Figure 45. Image. Area where V is greater than $0.867V_{max}$ at the outlet for $Q/A_o = 69$ cm/s (27 inches/s).
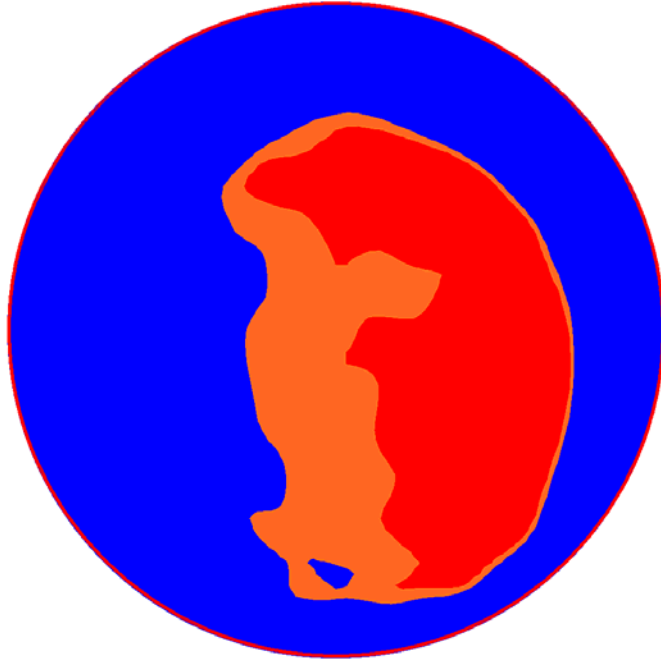
Figure 46. Image. Area where V is greater than $0.90V_{max}$ at the outlet for $Q/A_o = 69$ cm/s (27 inches/s).
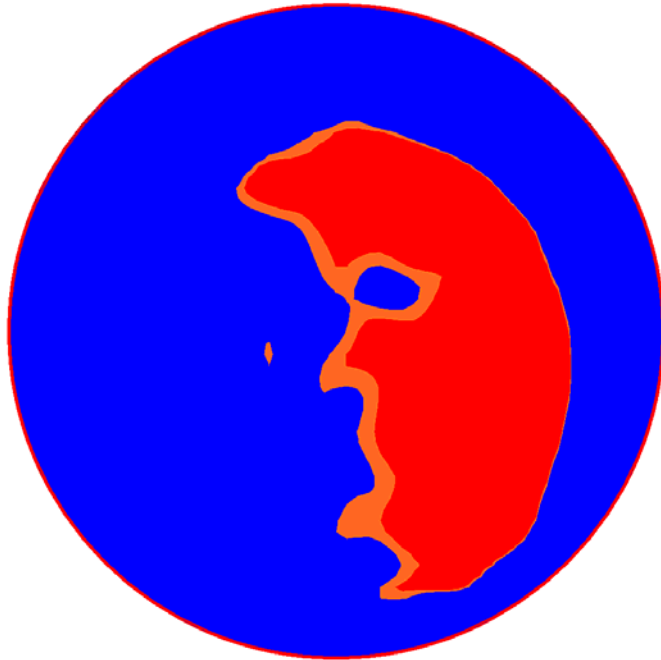
Figure 47. Image. Area where V is greater than $0.925V_{max}$ at the outlet for $Q/A_o = 69$ cm/s (27 inches/s).

APPENDIX C. VELOCITY PROFILES USED IN THE ACCESS HOLE RUNS

The following images show the velocity profile in the outflow pipe from the access hole experiments. These were used to validate K_i. Blue indicates low velocity, while the spectrum toward red reflects increasing magnitudes of local velocity.
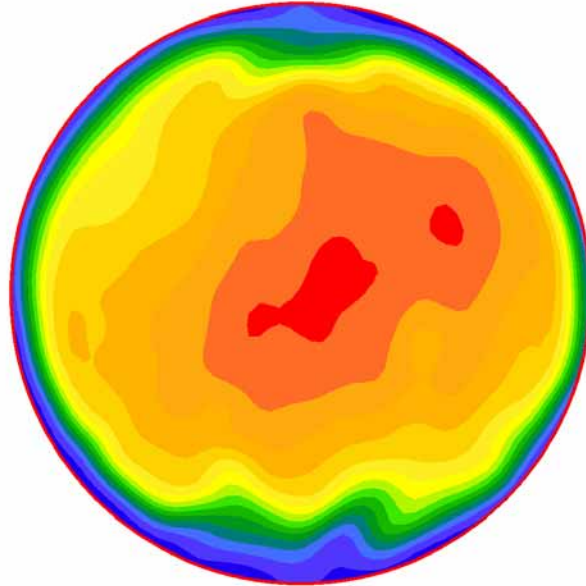
Figure 48. Image. Velocity profile 5 mm (0.19 inch) from the outlet for $Q/A_o = 43$ cm/s (17 inches/s).
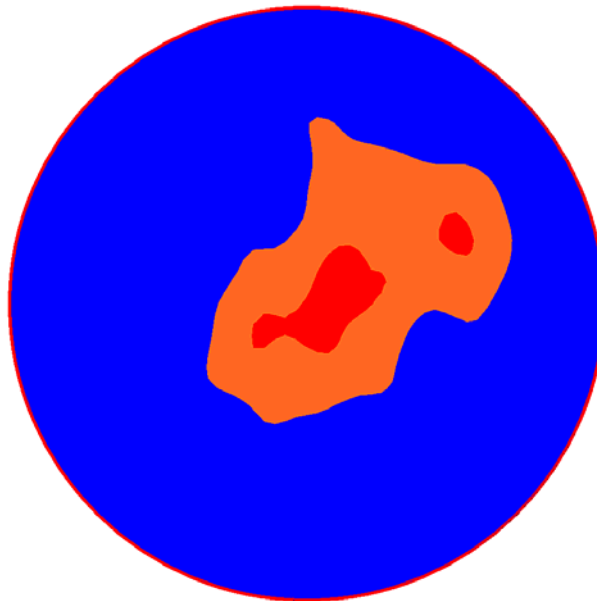
Figure 49. Image. Area where V is greater than $0.867V_{max}$ 5 mm (0.19 inch) from the outlet for $Q/A_o = 43$ cm/s (17 inches/s).
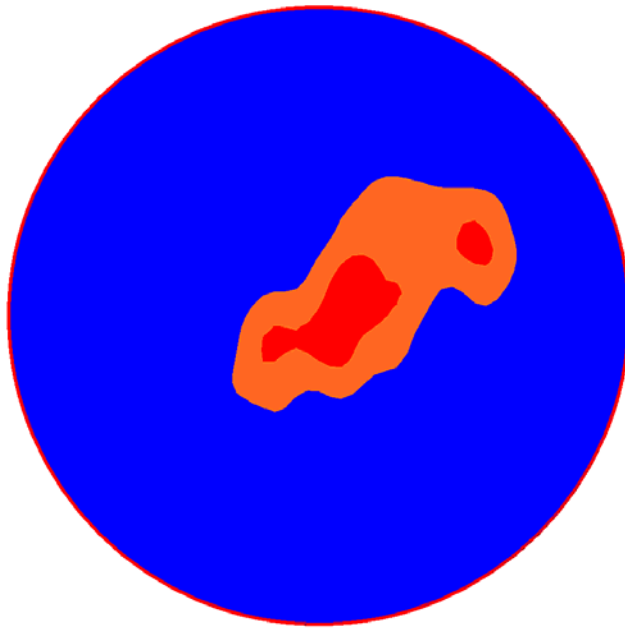
Figure 50. Image. Area where V is greater than $0.90V_{max}$ 5 mm (0.19 inch) from the outlet for Q/A_o = 43 cm/s (17 inches/s).
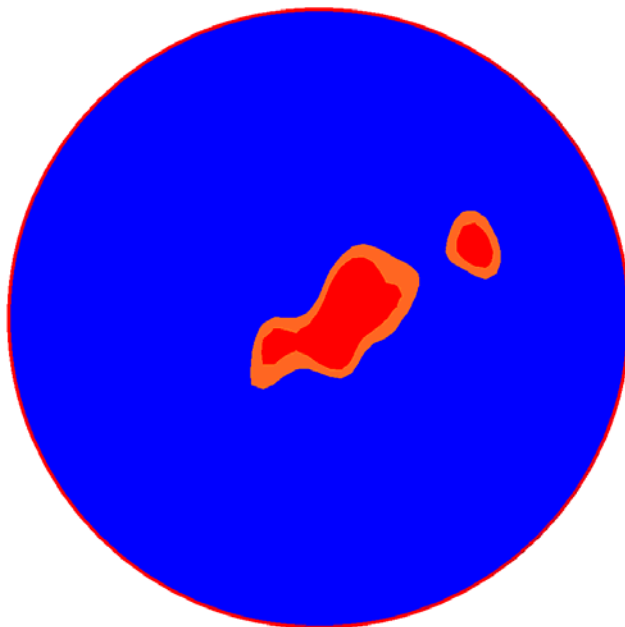
Figure 51. Image. Area where V is greater than $0.925V_{max}$ 5 mm (0.19 inch) from the outlet for Q/A_o = 43 cm/s (17 inches/s).
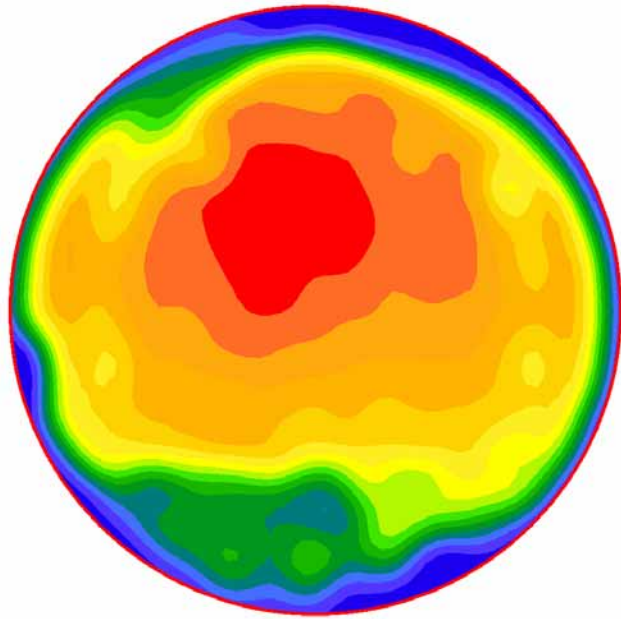
Figure 52. Image. Velocity profile at the outlet for Q/A_o = 57 cm/s (22 inches/s).
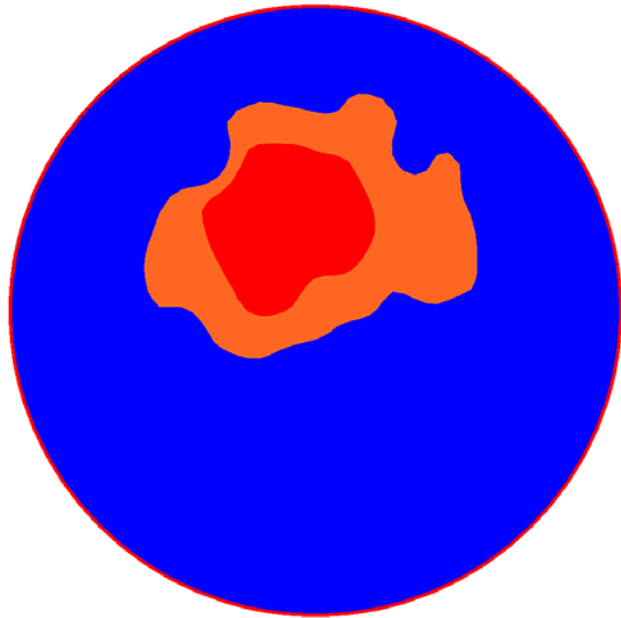
Figure 53. Image. Area where V is greater than $0.867V_{max}$ at the outlet for Q/A_o = 57 cm/s (22 inches/s).
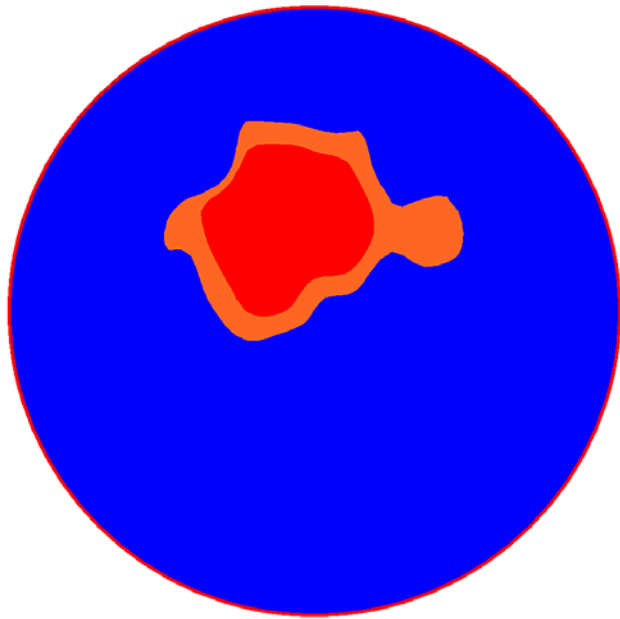
Figure 54. Image. Area where V is greater than 0.90V$_{max}$ at the outlet for Q/A$_o$ = 57 cm/s (22 inches/s).
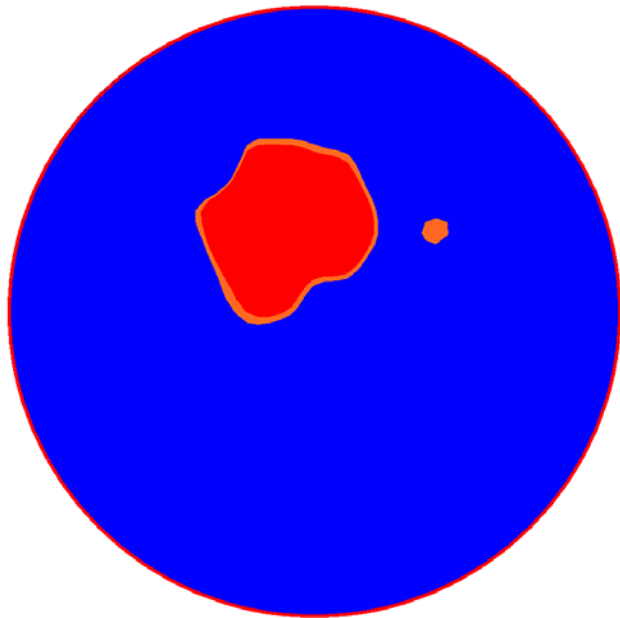
Figure 55. Image. Area where V is greater than 0.925V$_{max}$ at the outlet for Q/A$_o$ = 57 cm/s (22 inches/s).
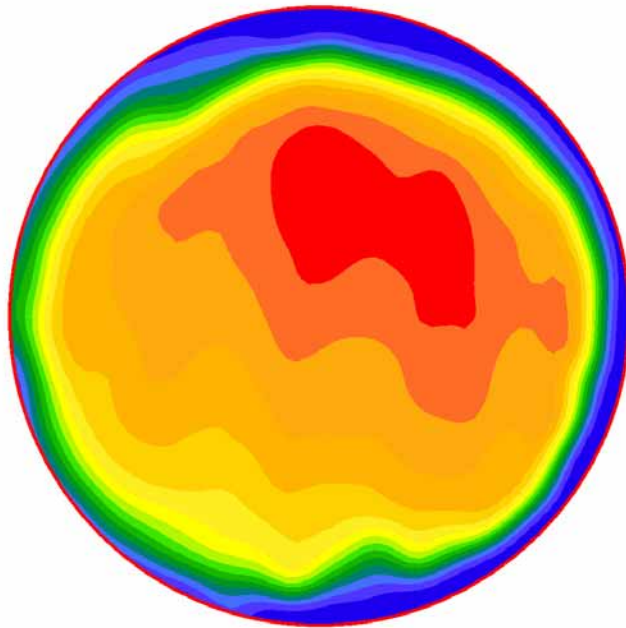
Figure 56. Image. Velocity profile at the outlet for Q/A_o = 64 cm/s (25 inches/s).
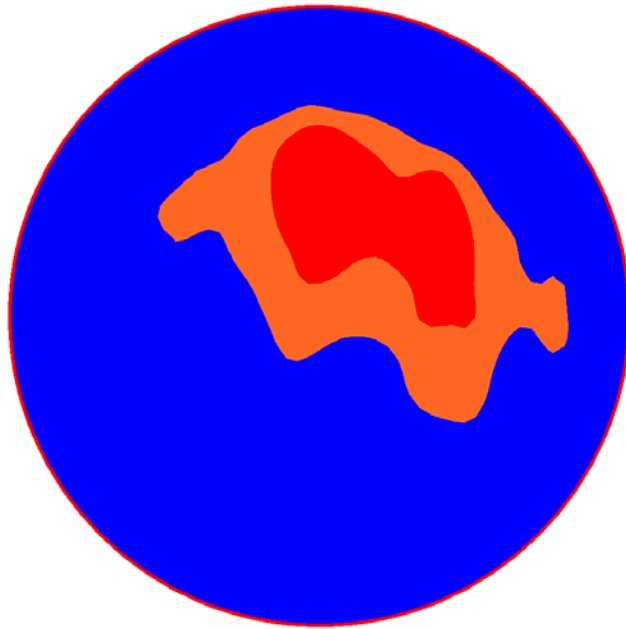
Figure 57. Image. Area where V is greater than $0.867V_{max}$ at the outlet for Q/A_o = 64 cm/s (25 inches/s).
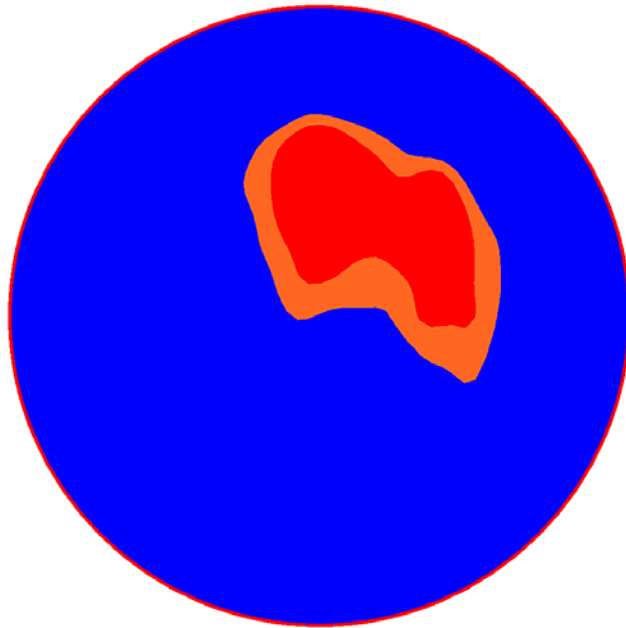
Figure 58. Image. Area where V is greater than 0.90V_{max} at the outlet for Q/A$_o$ = 64 cm/s (25 inches/s).
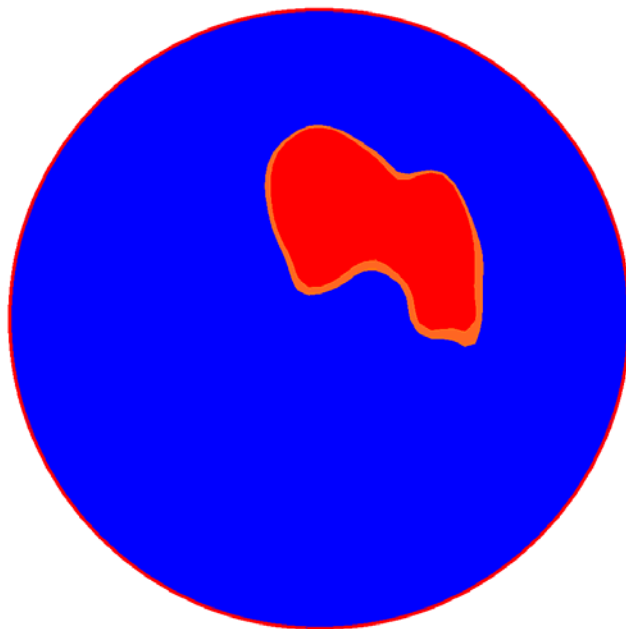
Figure 59. Image. Area where V is greater than 0.925V_{max} at the outlet for Q/A$_o$ = 64 cm/s (25 inches/s).
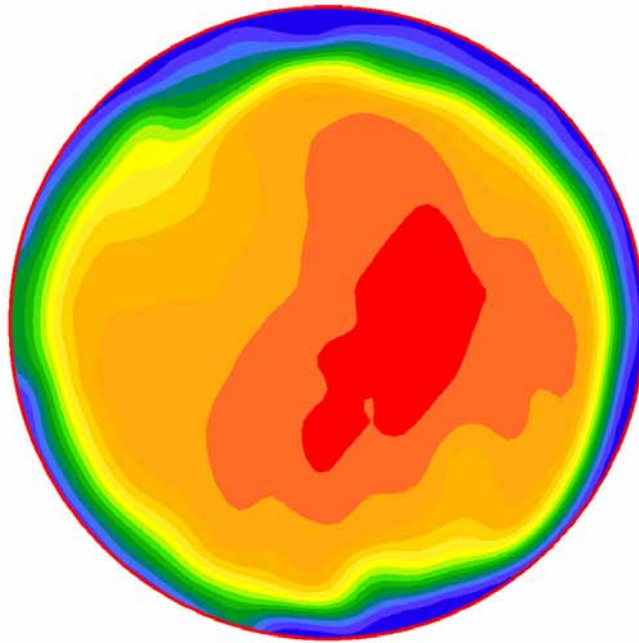
Figure 60. Image. Velocity profile at the outlet for Q/A_o = 75 cm/s (30 inches/s).
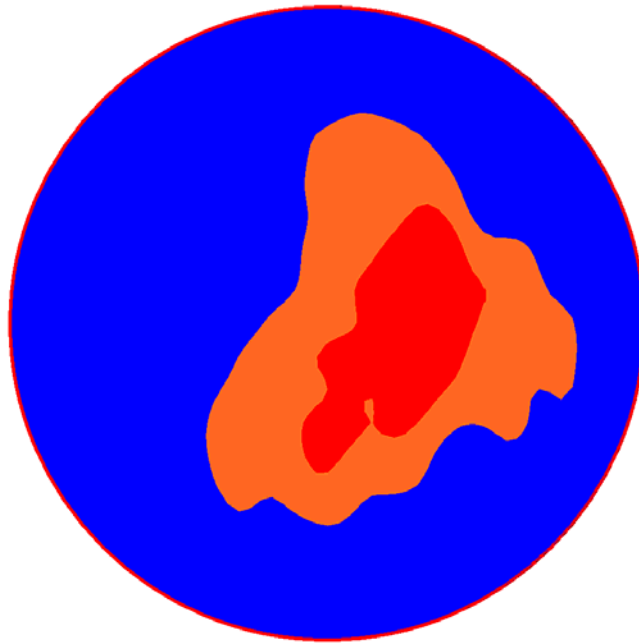
Figure 61. Image. Area where V is greater than $0.867V_{max}$ at the outlet for Q/A_o = 75 cm/s (30 inches/s).
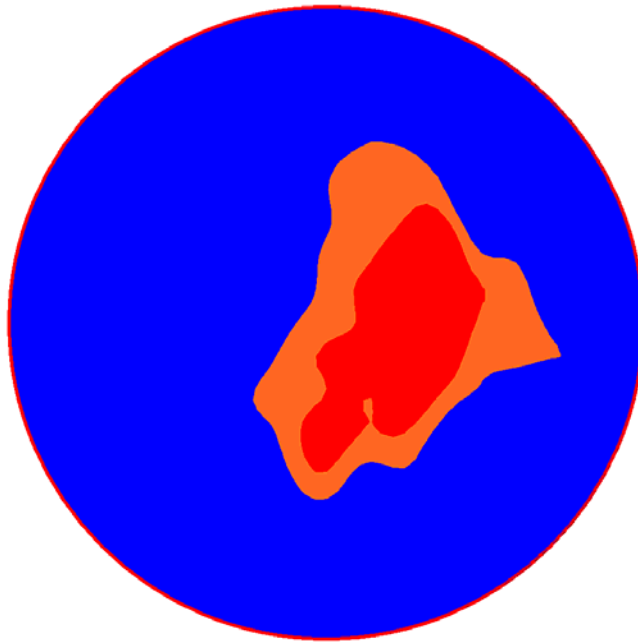
Figure 62. Image. Area where V is greater than $0.90V_{max}$ at the outlet for $Q/A_o = 75$ cm/s (30 inches/s).
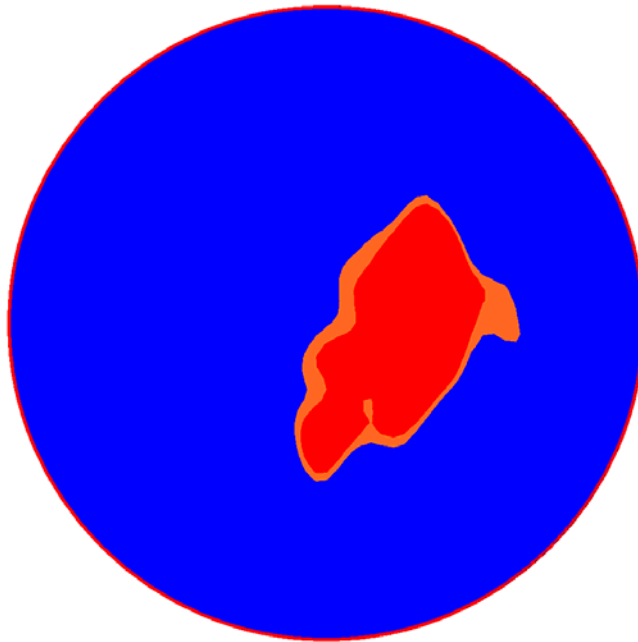
Figure 63. Image. Area where V is greater than $0.925V_{max}$ at the outlet for $Q/A_o = 75$ cm/s (30 inches/s).

REFERENCES

1. Chang, F.M., R.T. Kilgore, D.C. Woo, and M.P. Mistichelli, *Energy Losses through Junction Manholes*, FHWA-RD-94-080, Federal Highway Administration, Washington, DC, 1994.

2. Brown, S.A., S.M. Stein, J.C. Warner, *Urban Drainage Design Manual*, 2nd Ed., Hydraulic Engineering Circular No. 22, FHWA-NHI-01-021, National Technical Information Service, Springfield, VA, 2001.

3. Young, G. Kenneth, D.R. Pearson, S.M. Stein, J.S. Krolak, and A.T. Atayee, *HYDRAIN Integrated Drainage Design Computer System (version 6)*, FHWA-SA-96-064, Washington, DC, 1996.

4. Kilgore, R.T., *A Proposed Storm Drain Energy Loss Methodology for Access Holes*, unpublished research report, January 27, 2006.

5. Marsalek, J., *Head Losses at Selected Sewer Manholes*, American Public Works Association, Special Report 52, Chicago, IL, 1985.

6. Sangster, W.M., H.W. Wood, E.T. Snerdon, and H.G. Bossy, *Pressure Changes at Storm Drain Junctions*, Engineering Series, Bulletin 41, Engineering Experiment Station, University of Missouri, Columbia, MO, 1958.

7. Norman, J.M., R.J. Houghtalen, and W.J. Johnston, *Hydraulic Design of Highway Culverts (HDS 5)*, FHWA-NHI-01-020, National Technical Information Service, Springfield, VA, 2001.

8. Morris, H.M., *Applied Hydraulics in Engineering*, The Ronald Press Company, New York, NY, 1963.